

Evaluating the Relationships Between NTNU/SINTEF Drillability Indices with Index Properties and Petrographic Data of Hard Igneous Rocks

Saeed Aligholi¹ · Gholam Reza Lashkaripour¹ · Mohammad Ghafouri¹ · Sadegh Tarigh Azali¹

Received: 8 November 2016 / Accepted: 23 July 2017 / Published online: 31 July 2017
© Springer-Verlag GmbH Austria 2017

Abstract Thorough and realistic performance predictions are among the main requisites for estimating excavation costs and time of the tunneling projects. Also, NTNU/SINTEF rock drillability indices, including the Drilling Rate IndexTM (DRI), Bit Wear IndexTM (BWI), and Cutter Life IndexTM (CLI), are among the most effective indices for determining rock drillability. In this study, brittleness value (S_{20}), Sievers' J-Value (SJ), abrasion value (AV), and Abrasion Value Cutter Steel (AVS) tests are conducted to determine these indices for a wide range of Iranian hard igneous rocks. In addition, relationships between such drillability parameters with petrographic features and index properties of the tested rocks are investigated. The results from multiple regression analysis revealed that the multiple regression models prepared using petrographic features provide a better estimation of drillability compared to those prepared using index properties. Also, it was found that the semiautomatic petrography and multiple regression analyses provide a suitable complement to determine drillability properties of igneous rocks. Based on the results of this study, AV has higher correlations with studied mineralogical indices than AVS. The results imply that, in general, rock surface hardness of hard igneous rocks is very high, and the acidic igneous rocks have a lower strength and density and higher S_{20} than those of basic rocks. Moreover, DRI is higher, while BWI is lower in acidic igneous rocks, suggesting that drill and blast tunneling is more convenient in these rocks than basic rocks.

Keywords Igneous rock · Drillability · NTNU/SINTEF · Semiautomatic petrography · Index properties · Multivariate regression analysis

List of symbols

g	Index of interlocking
t	Index of grain size homogeneity
IS	Saturation Index
IF	Feldspathic Index
IC	Coloration Index
ρ	Dry density
ϕ	Porosity
V_p	P-wave velocity
R_N	Schmidt rebound number
$Is_{(50)}$	Point load strength index
S_{20}	Brittleness value
SJ	Sievers' J-Value
AV	Abrasion Value
AVS	Abrasion Value Cutter Steel
DRI	Drilling Rate Index
BWI	Bit Wear Index
CLI	Cutter Life Index
VHNR TM	Vickers Hardness Number Rock Trademark

1 Introduction

Tunneling and constructing underground spaces is a fundamental issue in transportation (roads, railways, and subway), industry (water transport, sewer system, and underground shelter), and mining (exploration, extraction, and drainage). Moreover, tunneling in rock masses is an inevitable necessity that imposes enormous costs on contractors without having sufficient knowledge. Thus, before

✉ Gholam Reza Lashkaripour
lashkaripour@um.ac.ir

¹ Department of Geology, Faculty of Science, Ferdowsi University of Mashhad, Mashhad, Iran

starting drilling operations, estimation of properties related to rock drillability to determine the properties of cutting tools and drilling machines' parts is necessary and useful as it leads to a reduction in drilling time and cost of the project. Nowadays, producing reliable and robust prognoses on cutter wear, drilling progress, and related costs is a highly sensitive issue for machine manufacturers and contractors dealing with the operation of mechanical excavation systems in mining, tunneling, and underground construction (Dahl et al. 2012).

Drill and blast (D&B) tunneling and tunnel boring machine (TBM) tunneling are the two dominating excavation methods in hard rock tunneling (Zare et al. 2016). In recent years, several researchers have extensively studied the parameters effective in rock excavation (Bruland 1998a; Barton 2000; Barla and Pelizza 2000; Blindheim et al. 2002; Yagiz 2002; Thuro and Plinninger 2003; Rostami et al. 2005; Villeneuve 2008; Hassanpour 2009; Farrokhi et al. 2011; Espallargas et al. 2015) and provided prognosis models for both D&B and TBM tunneling (Johannessen et al. 1995; Rostami 1997; Thuro 1997; Bruland 1998b; Dahl et al. 2007; Zare 2007; Yagiz 2008; Gong and Zhao 2009; Zhao et al. 2012; Hassanpour et al. 2014; Ellecosta et al. 2015).

The Norwegian University of Science and Technology (NTNU, former NTH) has a long history of developing prognosis models for the heavy construction industries (Macias et al. 2014a). These models comprise D&B tunneling time and cost, hard rock TBM time, tool life and cost, soft ground TBM tool life, and rock quarrying capacities and cost (Bruland 1998a; Zare and Bruland 2013; Jakobsen et al. 2013). The models proposed by NTNU may be used through all phases of tunneling projects for economic dimensioning, choice of alternative, time planning, cost analysis, and choice of excavation method and equipment (Zare et al. 2016).

In this study, drillability properties are evaluated for a wide range of igneous rocks in Iran using NTNU/SINTEF methods, which are among the most successful models for determining rock drillability. Moreover, because the direct determination of these properties involves conducting time-consuming and expensive tests and requires special equipment, evaluating the effect of index properties as well as petrographical features on drillability properties is among the main objectives of this work. In addition, the feasibility study of indirect methods, in order to provide reliable estimates of these parameters, is of high importance in this research. For this purpose, after determining drillability properties and physical, the mechanical, and petrographical characteristics of the samples, the relationships between these parameters were studied, and some optimum methods were proposed based on statistical analyses to estimate the drillability characteristics of the studied rocks.

The Drilling Rate IndexTM (DRI), Bit Wear IndexTM (BWI), and Cutter Life IndexTM (CLI) are registered trademarks of the Foundation for Scientific and Industrial Research (SINTEF) and NTNU in Trondheim, Norway (Dahl et al. 2010). For the sake of readability, the trademark symbol is omitted in the rest of manuscript.

2 Experimental Material

This research is aimed to inquire the relationships between petrographic features as well as index properties with NTNU/SINTEF drillability parameters of hard igneous rocks. For such a purpose, based on a preliminary desk study as well as the macroscopic structure and visible features, a total of 28 hard igneous rocks were sampled at 15 different locations in Iran. A wide range of hard igneous rocks including granitoid, dacite, diorite, andesite, gabbro, and basalt were examined in this study (Table 1). According to Anon (1995), all samples were unweathered or slightly weathered. Blocks were carefully checked to ensure they are homogeneous and free from visible weaknesses. Each block sample was drilled or cut to obtain cylindrical cores or blocks specimens for inspecting engineering properties. Also, thin sections were prepared from each rock sample for petrographic analysis.

3 Petrography

Rocks are mostly composed of varying percentages of minerals with different textural properties such as grain size, grain shape, and microfabric characteristics. Some rock properties which highly affect the progress rate and the equipment in mining, tunneling, and underground construction are mineralogy, texture, grain shape, grain binding, and grain size (Dahl et al. 2007). Many researchers dealt with the relationship between petrographic features and mechanical behavior of different rocks (Hugman and Friedman 1979; Howarth and Rowlands 1987; Ulusay et al. 1994; Ersoy and Waller 1995; Tugrul and Zarif 1999; Prikryl 2006; Tandon and Gupta 2013; Hashemnejad et al. 2016; Moradzadeh et al. 2016). However, the relations between the petrographic features and the NTNU/SINTEF rock drillability properties have not been investigated in detail yet.

In this research, we study the effects of petrographic characteristic including texture features and mineral composition on drillability properties of igneous rocks. The procedure planned for the quantitative analysis of the petrographic features is relatively simple: producing representative images using digital microscopy, preprocessing

Table 1 Modal analysis and the names of the studied rocks

Rock code	Qtz (%)	Pl (%)	Afs (%)	Bt (%)	Ms (%)	Am (%)	Chl (%)	Cpx (%)	Opx (%)	Ol (%)	Grt (%)	OM (%)	Ep (%)	Gl (%)	AM <1%	Rock name*
R1	28	35	20	17	–	–	–	–	–	–	–	–	–	–	Zrn	Micro-monzogranite
R2	38	24	28	3	7	–	–	–	–	–	–	–	–	–	–	Monzogranite
R3	31	21	34	4	9	–	1	–	–	–	–	–	–	–	–	Monzogranite
R4	–	41	–	–	–	5	–	8	5	–	2	2	1	36	–	Hyalo-basaltic andesite
R5	32	34	27	4	–	2	–	–	–	–	–	1	–	–	–	Monzogranite
R6	–	47	–	–	–	4	–	19	5	9	–	13	3	–	–	Basalt
R7	37	22	31	7	–	1	2	–	–	–	–	–	–	–	Zrn	Monzogranite
R8	37	18	38	5	–	1	1	–	–	–	–	–	–	–	Zrn	Syenogranite
R9	41	14	40	2	–	1	2	–	–	–	–	–	–	–	Zrn	Syenogranite
R10	26	17	48	6	–	–	1	–	–	–	–	–	2	–	–	Syenogranite
R11	12	34	7	9	–	3	–	–	–	–	–	3	–	32	–	Hyalo-dacite
R12	29	38	22	4	–	3	2	–	–	–	1	1	–	–	–	Monzogranite
R13	14	46	16	–	–	12	9	–	–	–	–	3	–	–	Zrn	Quartz-Monzodiorite
R14	12	59	3	–	–	7	9	4	–	–	–	6	–	–	–	Quartz-Andesite
R15	1	64	1	3	–	23	3	–	–	–	1	4	–	–	Spn	Diorite
R16	4	63	6	–	–	14	8	–	–	–	–	5	–	–	–	Andesite
R17	28	29	35	5	–	–	3	–	–	–	–	–	–	–	–	Monzogranite
R18	–	48	–	4	–	3	–	16	6	–	9	6	8	–	–	Gabbro
R19	–	36	–	5	–	7	–	18	11	14	–	2	7	–	–	Gabbro
R20	–	57	2	4	–	6	–	–	11	8	1	5	6	–	Zrn	Diorite
R21	–	58	3	4	–	4	–	13	3	7	1	4	3	–	–	Diorite
R22	13	33	41	1	–	9	–	–	–	–	–	3	–	–	–	Quartz-Monzonite
R23	7	40	44	1	–	6	–	–	–	–	–	2	–	–	–	Quartz-Monzonite
R24	12	24	56	2	–	4	–	–	–	–	–	2	–	–	–	Quartz-Syenite
R25	3	69	7	4	–	14	–	–	–	–	–	3	–	–	–	Andesite
R26	27	41	19	6	–	4	1	–	–	–	–	2	–	–	Spn	Granodiorite
R27	29	45	9	7	–	6	2	–	–	–	1	1	–	–	Spn	Granodiorite
R28	–	59	–	8	–	5	–	12	4	–	–	2	6	4	–	Micro-gabbro

Qtz Quartz, Pl Plagioclase, Afs Alkali feldspar, Bt Biotite, Ms Muscovite, Am Amphibole, Chl Chlorite, Cpx Clino pyroxene, Opx Orthopyroxene, Ol Olivine, Grt garnet, OM Opac minerals, Ep Epidote, Gl glass, AM Accessory minerals, Zrn zircon, Spn Sphene

* According to optical microscopy studies (Streckeisen 1976)

and segmentation of images, and extracting petrographic feature.

3.1 Image Acquisition

In any consideration of the accuracy of micrometric analyses, there exists two distinct types of error which may enter into the results: (1) errors caused by failure of the measuring process to give an adequate representation of the thin section to which it is applied and (2) errors due to

failure of the thin section to provide a proper sample of the rock from which it is cut (Larsen and Miller 1935). In this study, depending on grain size, the variations in grain size, and rock homogeneity, different numbers of thin sections were prepared for each studied rock. Then, thin sections were imaged using a digital camera mounted on a petrographic microscope. Measurement of 50–200 grains is often needed in order to adequately characterize a thin section (Middleton et al. 1985). Considering the grain size and homogeneity of the studied thin sections, different

methodologies are employed for producing representative images. For coarse-grained rocks, the mosaics of the photomicrographs were generated by stitching together the photomicrographs through selected scan lines from representative parts of thin sections. An example of these mosaics for the photomicrographs obtained from some studied coarse-grained rocks is shown in Fig. 1. For fine-grained rocks, depending on their homogeneity, images were taken from 1 to 5 parts of their thin sections. For example, the photomicrographs obtained from thin sections of the R1 sample are shown in Fig. 2a.

3.2 Image Analysis and Feature Extraction

Combining thin section examination with computer programs that analyze rock photomicrograph is a standard procedure in geology (Petruk 1989) since such programs allow fast measurement and quantitative analysis of thin-section features (Reedy 2006). Several image processing and pattern recognition techniques such as color analysis and textural analysis are employed in mineralogy. Most of such techniques are devoted to the field of rock analysis, especially to quantify the crystal/grain size distributions and crystal/grain shapes (Aligholi et al. 2015). A number of petrographic image segmentation techniques such as threshold, boundary-based, region-based, and hybrid techniques are found in the literature (e.g., Zhou et al. 2004; Fueten and Mason 2007; Asmussen et al. 2015; Izadi et al. 2015). Segmentation of rock photomicrographs allows to quantify the inner structure of the specimen, that is, the number of grains per mineral, their sizes, shapes or relative orientations, etc. (Aligholi et al. 2017a).

In this study, petrographic images were segmented using a method that relies on three main steps: preprocessing, automated segmentation, and manual post-processing. The preprocessing step involves converting RGB images to grayscale and image enhancement. The image enhancement involves two noise reduction cycles using a median filter, enhancing the contrast of images using histogram equalization, and opening—losing by reconstruction which uses the fast hybrid grayscale reconstruction algorithm described in (Vincent 1993). Such morphological operations reduce the negative effects of noise within grain regions (e.g., cracks, twinning, and undulose extinction) while retaining the shape of the grains is of much interest.

To segment grains in rocks under examination, an algorithm described by Jin (2012) was employed. The method has four main steps: (1) computing a gradient map or intensity map from the image; (2) computing a cumulative distribution function from the gradient map; (3) modifying the map using the selected scale level value; and (4) segmenting the modified gradient map using a watershed transform.

Since the textural features of some minerals (such as plagioclase and microcline), which commonly show twinning, cause a faulty segmentation of these minerals, a post-processing step is essential.

To extract petrographic features, the segmented photomicrographs were firstly scaled by converting the pixel values into the millimeter unit by a conversion factor obtained using a standard scaled thin section for each microscope magnification. Next, the basic size and shape descriptors as introduced in Table 2 were computed for each grain of tested rocks, followed by averaging the size and shape descriptors of all grains for each rock for further investigations (Table 3). It is notable that for each rock sample the mean orientation of all grains was subtracted from 90° and the absolute of this number was reported as the orientation value. The higher values of this parameter show that the grains of a given rock are more oriented along a specific direction. It also worth mentioning that the images were taken in a direction with the visual principle orientation of rocks grain for the possible biases around 90°. However, grains of the studied igneous rocks are not generally oriented to a specific direction. As presented in Table 1, the modal composition of the studied rocks was obtained using manual classification of segmented grains as shown in Fig. 2b, c.

Based on such basic size and shape descriptors, two rock fabric coefficients, namely index of interlocking and index of grain size homogeneity, were computed for each studied rock (Table 4) as follows.

Index of interlocking (g) is an arithmetic mean of the proportion of rock grains perimeter which contacts neighboring grains quantified by the square root of their respective area Dreyer (1973). The increasing value of this parameter indicates a higher complexity of the grains' boundaries, suggesting that the grain boundaries are more lobate (Prikrýl 2006). This index is computed from the following formulas:

$$g = \frac{1}{n} \cdot \sum \frac{L_{pi}}{\sqrt{A_i}} \quad (3.1)$$

where n is the number of grains considered, while L_{pi} and A_i are the grain perimeter which contacts neighboring grains and grain area, respectively. Here, the index of interlocking of samples R4 and the R11 are considered as zero because these samples are two hyaline extrusive rocks and their grains mostly do not contact with each other.

Index of grain size homogeneity (t) is a fabric parameter that describes the grain size distribution in the material (Dreyer 1973):

$$t = \frac{A_{avg}}{\sqrt{\sum (A_i - A_{avg})^2}} \quad (3.2)$$

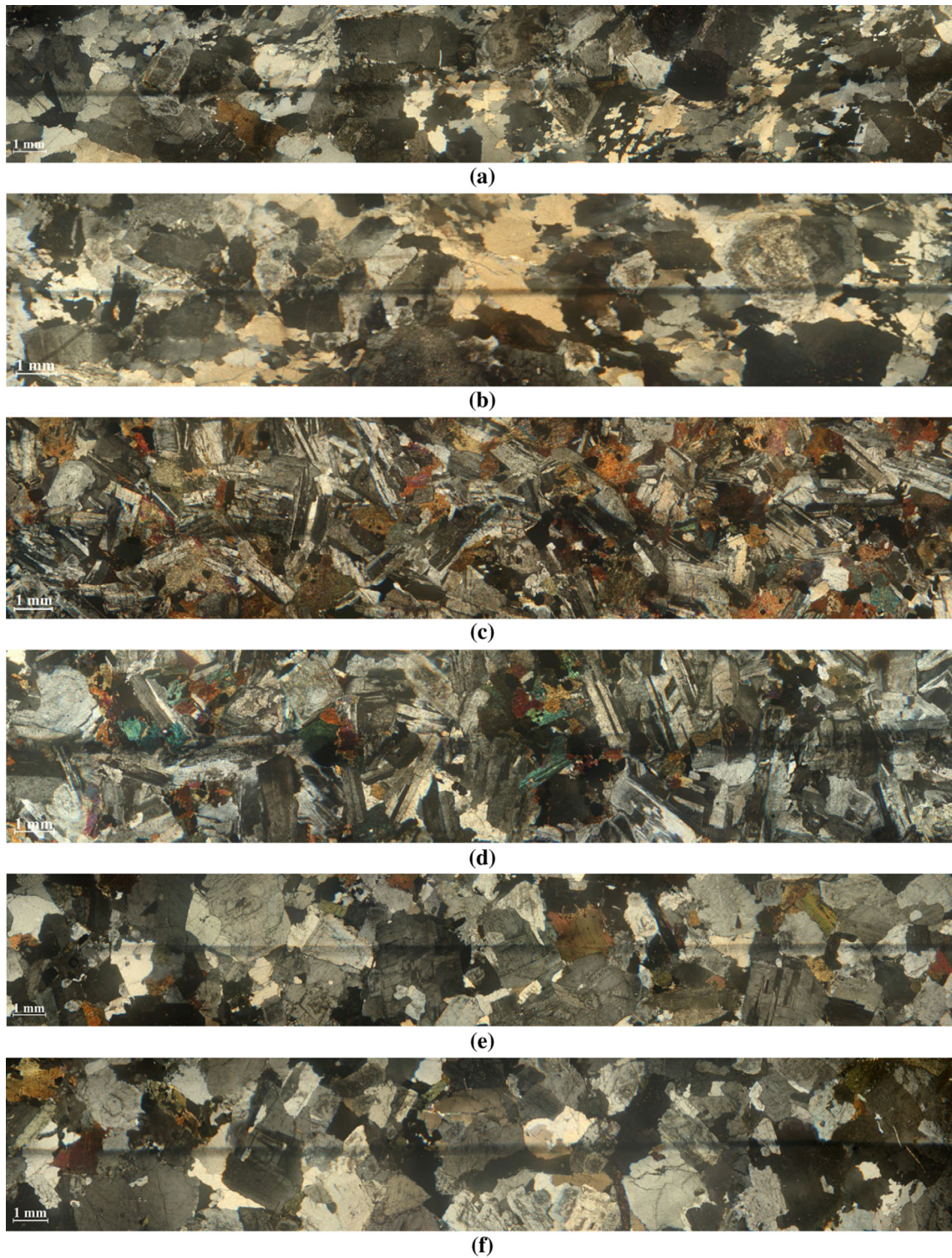


Fig. 1 Mosaics from thin sections of samples R9 (a–b), R15 (c–d), and R26 (e–f). Note that the selected scan lines to create representative images are shown using a pencil

where A_{avg} is the average area of the grains and A_i is the area of individual grain.

In addition, some mineralogical indices used in the modal classification of igneous rocks (Jung and Brousse

1959) were extracted using modal analysis of the rocks. The results are given in Table 4. While the mineralogical indices are presented as follows.

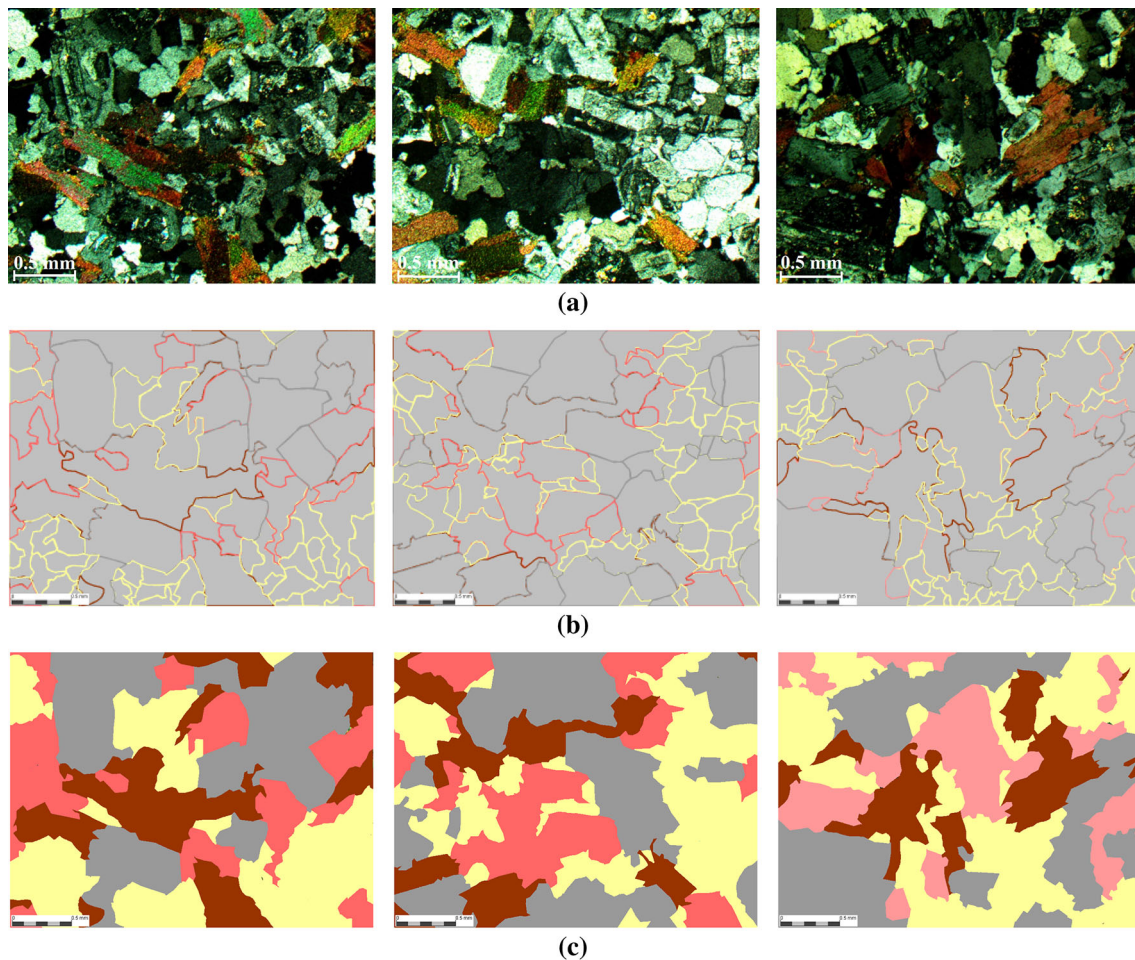


Fig. 2 Analyzed photomicrographs from representative images of thin sections for sample R1 (a); segmented maps of images shown in a (b); and polygon maps of images shown in a (c)

Table 2 Summary of the studied basic size and shape descriptors

Category	Parameter	Computation
Size descriptor	Area	Number of pixels in the object
	Perimeter	Length of the outline of the object
	Size	Equivalent circular diameter
	Minimum Feret's diameter	Minimum caliper
	Maximum Feret's diameter	Maximum caliper
Shape descriptor	Elongation	Ratio of the maximum to the minimum Feret's diameter
	Orientation	Angle between the horizontal axis and the major axis of the ellipse equivalent to the object (0–180°, counterclockwise)
	Eccentricity	Ratio between the major and the minor axis of the ellipse equivalent to the object
	Compactness	Ratio of the area of the object to the area of a circle with the same perimeter
	Rectangularity	Ratio of the area of a rectangle (formed with length and width as sides) to the area of the object
	Solidity	Ratio of the area of the object to the area of the convex hull of the object
	Convexity	Ratio of the perimeter of the convex outline of the object to the perimeter of the object

Table 3 Basic size and shape descriptors of the studied rocks

Rock code	Area (mm ²)	Perimeter (mm)	Size (mm)	Min of Feret's (mm)	Max of Feret's (mm)	Elongation	Orientionation (°)	Eccentricity	Compactness	Rectangularity	Solidity	Convexity
R1	0.07	1.59	0.27	0.26	0.44	1.70	1.40	4.48	0.36	1.04	0.71	0.78
R2	0.55	4.83	0.75	0.70	1.24	1.76	1.28	4.39	0.28	1.04	0.72	0.69
R3	0.47	4.34	0.67	0.64	1.08	1.68	1.69	3.91	0.30	1.02	0.71	0.70
R4	0.35	3.42	0.58	0.54	0.92	1.72	7.04	4.53	0.37	0.94	0.75	0.76
R5	0.51	4.55	0.67	0.63	1.14	1.81	10.44	4.27	0.32	1.04	0.71	0.73
R6	0.01	0.46	0.09	0.08	0.13	1.65	0.39	3.21	0.54	0.67	0.76	0.84
R7	0.54	4.68	0.66	0.63	1.11	1.77	3.70	4.92	0.28	1.06	0.70	0.70
R8	0.79	5.34	0.78	0.74	1.31	1.77	8.19	4.61	0.29	1.07	0.70	0.70
R9	0.59	4.88	0.71	0.66	1.23	1.86	10.50	5.23	0.29	1.07	0.70	0.71
R10	1.56	6.90	0.91	0.84	1.56	1.85	7.21	5.75	0.30	1.08	0.71	0.71
R11	0.23	2.81	0.47	0.44	0.78	1.78	2.85	4.52	0.37	0.97	0.73	0.77
R12	0.43	4.19	0.64	0.63	1.06	1.68	5.98	3.96	0.31	1.05	0.70	0.72
R13	0.18	2.84	0.43	0.41	0.72	1.77	8.99	5.35	0.29	1.12	0.70	0.72
R14	0.13	2.37	0.33	0.32	0.57	1.79	0.33	4.86	0.28	1.21	0.67	0.70
R15	0.57	5.35	0.74	0.72	1.33	1.86	9.97	6.39	0.26	1.19	0.68	0.69
R16	0.09	2.07	0.30	0.28	0.52	1.83	8.00	5.27	0.29	1.20	0.67	0.72
R17	1.05	6.68	0.97	0.92	1.62	1.77	12.21	4.67	0.28	1.06	0.71	0.68
R18	0.17	2.70	0.41	0.39	0.67	1.71	2.64	4.41	0.27	1.17	0.69	0.69
R19	0.16	2.83	0.40	0.39	0.69	1.78	10.53	5.25	0.26	1.20	0.68	0.69
R20	0.25	3.19	0.47	0.44	0.80	1.81	9.83	5.35	0.29	1.13	0.70	0.71
R21	0.29	3.84	0.53	0.50	0.92	1.83	2.54	5.13	0.25	1.19	0.67	0.67
R22	1.08	6.66	0.92	0.86	1.61	1.87	10.97	5.35	0.27	1.06	0.71	0.69
R23	1.16	7.60	0.98	0.94	1.69	1.80	7.64	4.58	0.24	1.14	0.69	0.65
R24	1.83	9.09	1.21	1.18	2.04	1.73	10.12	5.05	0.27	1.10	0.71	0.67
R25	0.02	0.93	0.13	0.12	0.24	1.93	19.29	5.49	0.26	1.16	0.67	0.69
R26	1.06	6.71	1.03	0.97	1.67	1.74	2.39	4.54	0.30	0.98	0.73	0.70
R27	1.20	6.33	0.99	0.91	1.61	1.77	1.08	4.78	0.31	0.99	0.74	0.72
R28	0.07	1.88	0.26	0.25	0.45	1.78	5.23	5.00	0.28	1.28	0.65	0.71

Table 4 Fabric coefficients and the mineralogical indices of the studied rocks

Rock code	Fabric coefficient		Mineralogical index		
	<i>g</i>	<i>T</i>	IS	IF	IC
R1	6.33	0.064	33.73	36.36	17
R2	7.07	0.056	42.22	53.85	10
R3	6.92	0.051	36.05	61.82	14
R4	0	0.043	0.00	0.00	36
R5	6.80	0.047	34.41	44.26	7
R6	5.17	0.022	0.00	0.00	53
R7	7.22	0.039	41.11	58.49	10
R8	7.11	0.038	39.78	67.86	7
R9	7.11	0.040	43.16	74.07	5
R10	7.21	0.036	28.57	73.85	9
R11	0	0.055	23.08	16.66	22
R12	6.81	0.050	32.58	36.67	11
R13	7.12	0.088	18.42	25.81	24
R14	7.45	0.035	16.22	4.84	26
R15	7.54	0.052	1.52	1.54	34
R16	7.27	0.047	5.48	8.70	27
R17	7.31	0.057	30.43	54.69	8
R18	7.28	0.071	0.00	0.00	52
R19	7.57	0.065	0.00	0.00	64
R20	7.15	0.060	0.00	3.39	41
R21	7.73	0.049	0.00	4.92	39
R22	7.34	0.041	14.94	55.41	13
R23	7.80	0.063	7.69	52.38	9
R24	7.62	0.079	13.04	70.00	8
R25	7.54	0.083	3.80	9.21	21
R26	6.97	0.083	31.03	31.67	13
R27	6.77	0.046	34.94	16.67	17
R28	7.54	0.033	0.00	0.00	39

Saturation Index (IS) is the ratio of the percentage of quartz (Qtz) to the summed percentage of quartz and feldspars:

$$IS = \frac{Qtz\%}{(Qtz + Afs + Pl)\%} \times 100 \quad (3.3)$$

Feldspathic Index (IF) is the ratio of the percentage of alkali feldspars (Afs) to summed percentage of alkali feldspars and plagioclase (Pl):

$$IF = \frac{Afs\%}{(Afs + Pl)\%} \times 100 \quad (3.4)$$

Coloration Index (IC) is the sum of volume percentages of the colored, or dark, minerals contained in the rock:

$$IC = 100 - (Qtz + Afs + Pl)\% \quad (3.5)$$

For the computation of mineralogical indices of hyaline rocks, the percentage of mineral phases is considered as 100.

4 Physicomechanical Properties

In order to assess the quality and engineering properties of studied hard igneous rocks, the index properties of rocks such as density, porosity, P-wave velocity, Schmidt hammer rebound hardness number, and point load strength index ($Is_{(50)}$) are determined based on laboratory tests. Each block sample was drilled or cut to obtain cylindrical cores or blocky specimens to inspect the physical, dynamic, and mechanical properties. Various standard test procedures were carried out to determine properties of the studied rocks. The basic physical properties of the rock samples including density and porosity were measured according to ISRM (1981). The P-wave velocity was determined using a Portable Ultrasonic Non-destructive Digital Indicating Tester (PUNDIT) according to ISRM (2007). Rebound hardness values of the rock samples were determined according to the procedure suggested by the ISRM (Aydin 2009) using an N-type Proceq Schmidt hammer on blocky samples while holding the hammer vertically downward and perpendicular to the horizontal rock faces. Point load strength test was performed on blocky or core samples (axial test) according to ISRM (1985). The results are shown in Table 5.

As shown in Table 5, the studied igneous rocks have generally a low porosity, high strength, and desirable engineering quality. Based on the results of laboratory tests, the acidic igneous rocks compared to basic igneous rocks indicate a lower density, P-wave velocity, and lower strength, and consequently a lower engineering quality. Nevertheless, the rebound hardness of igneous rocks is independent of their petrology.

5 NTNU/SINTEF Drillability Indices

NTNU/SINTEF rock drillability indices, i.e., DRI, BWI, and CLI, are indirect measures for the drillability of rocks, and represent important factors in connection with all kind of tunneling and rock excavation (Dahl 2003). These indices are determined based on brittleness, surface hardness, and abrasiveness of rock specimens using four laboratory tests namely, brittleness value (S_{20}), Sievers' J-Value (SJ), abrasion value (AV), and Abrasion Value Cutter Steel (AVS).

Brittleness is one of the most crucial rock features for rock excavation (Dursun and Gokay 2016). Brittleness

Table 5 Physiomechanical properties of the studied rocks

Rock code	Dry density (gr/cm ³)	Porosity (%)	P-Wave velocity (m/s)	SH rebound value (R_N)	Point load strength index $I_{s(50)}$ (MPa)
R1	2.72	1.13	4841	59.9	6.14
R2	2.63	1.01	4451	60.3	6.72
R3	2.62	1.25	4301	54.2	5.63
R4	2.65	0.65	5715	56.5	9.78
R5	2.64	1.4	5406	63.5	7.77
R6	2.91	0.89	6193	55.7	14.64
R7	2.63	0.87	5109	58.1	7.72
R8	2.62	0.86	5064	54.0	7.65
R9	2.62	0.84	5195	56.8	8.69
R10	2.69	0.76	5136	62.3	5.49
R11	2.59	1.91	5351	53.7	10.24
R12	2.64	1.49	4115	51.0	7.78
R13	2.72	2.76	4394	47.0	8.36
R14	2.75	0.57	6156	49.0	12.29
R15	2.89	0.67	5422	48.8	11.93
R16	2.69	1.26	5825	59.4	8.69
R17	2.62	1.31	4555	55.0	6.91
R18	2.98	0.55	6182	57.2	11.41
R19	3.14	0.18	7239	63.5	12.29
R20	2.83	0.18	6365	65.2	11.08
R21	2.78	0.26	6342	62.6	10.87
R22	2.58	2.31	5246	61.2	7.00
R23	2.63	1.46	5135	56.9	8.19
R24	2.56	3.57	4531	41.4	5.59
R25	2.64	0.74	5783	63.7	10.49
R26	2.66	1.07	4277	56.5	7.27
R27	2.65	1.19	5367	63.4	6.07
R28	2.89	0.29	6491	58.0	10.68

characteristics of rocks substantially affect their mechanical performance, drillability, cuttability, and machine performance (Aligholi et al. 2017b). So far, no internationally accepted norm has been proposed for measurement and determination of the rock brittleness. There are some definitions of brittleness for different purposes and various methods for determination of rock brittleness in the literature (Altindag 2010; Dursun and Gokay 2016). The brittleness test method, applied by NTNU/SINTEF, was originally developed in Sweden by von Matern and Hjelmner (1943). Although the original test was aimed to determine the strength properties of aggregates, several modified versions of the test have later been developed for various purposes. The version S_{20} of brittleness test, developed for the determination of rock drillability, has been used since the end of the 1950s (Dahl et al. 2012). An outline of the test is shown in Fig. 3a.

The Sievers' J-miniature (SJ) drill test (Sievers 1950) gives a measure of the surface hardness (or resistance against tool indentation) of the rock. The SJ-value is the depth of 4–8 drill holes after 200 revolutions of a miniature drill bit, measured in 1/10 mm. The basic principles of the test are shown in Fig. 3b.

The abrasivity is one of the important properties of rocks, which must be taken into consideration in drilling or excavation projects (Kahraman et al. 2016). As the wear life of the rock cutting tools often has a linear relationship with the measured rock abrasion, any variation in the measurements has a direct and proportional impact on the estimated tool life, operational delays, and related costs (Rostami et al. 2014). To estimate abrasiveness of rocks, several methods exist already, e.g., Vickers test, the Cerchar test, the LCPC abrasimeter test, and the NTNU abrasion test (Nilsen et al. 2007). Also, NTNU provides some methods for measuring AV and AVS. The AV test developed at the Department of

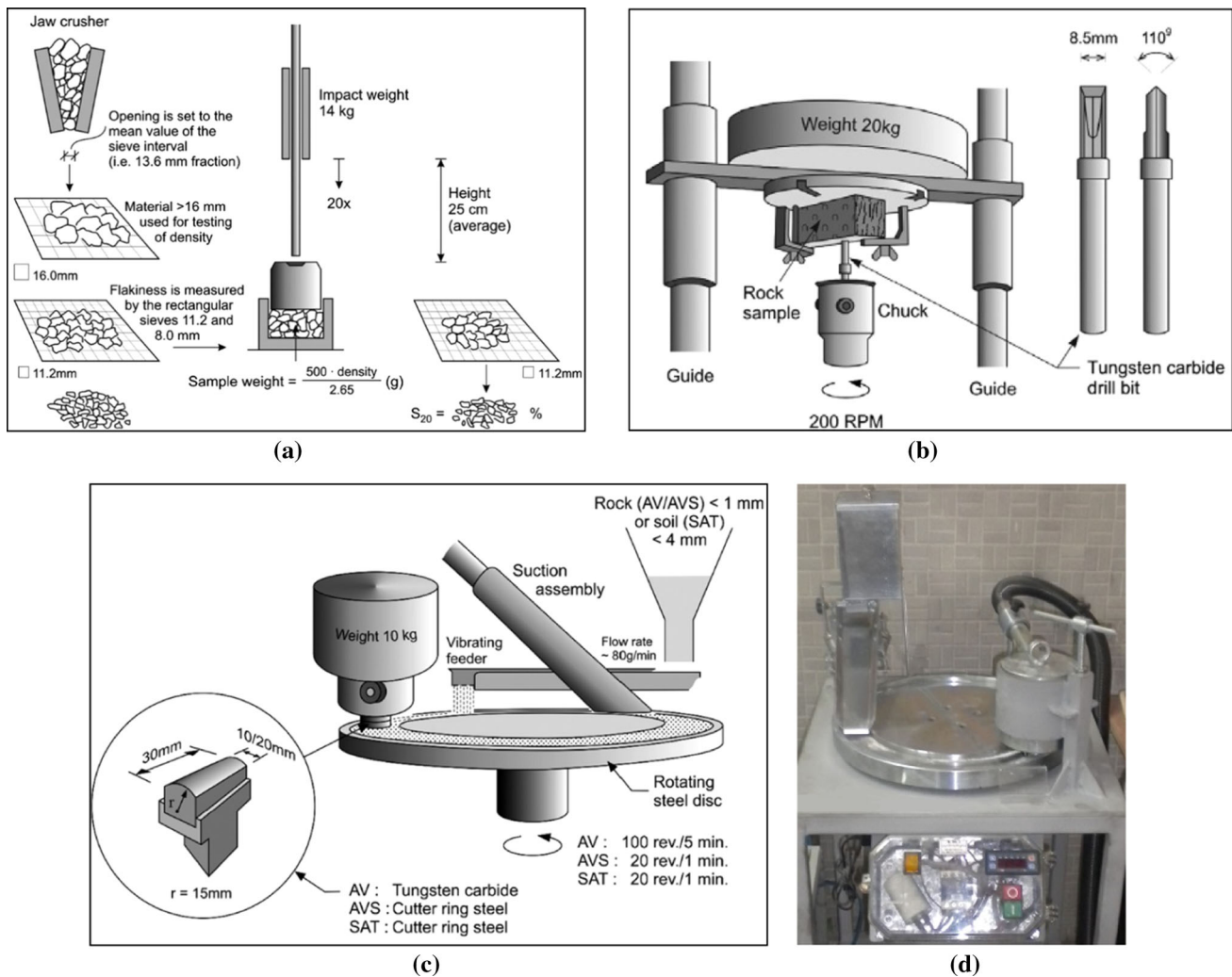


Fig. 3 Outlines of principles for the NTNU/SINTEF drillability test methods (Dahl et al. 2012): **a** Brittleness value (S_{20}) test; **b** Sievers' J-Value (SJ) miniature drill test; **c** abrasion value (AV) and Abrasion

Value Cutter Steel (AVS) test; and **d** the NTNU abrasion test apparatus in the Engineering Geology Laboratory of the Ferdowsi University of Mashhad (FUM)

Geology at NTH in the beginning of the 1960s constitutes a measure of the rock abrasion or ability to induce wear on tungsten carbide (Dahl et al. 2012). The AV is the weight loss in milligrams of the test bit after 100 revolutions of a steel disk. One hundred revolutions correspond to 5-min test time. The AVS, which was developed and introduced by NTNU in the early 1980s, constitutes a measure of rock abrasion or ability to induce wear on cutter ring steel (Macias et al. 2016). AVS, on the other hand, is measured by the same test equipment as the AV. The AVS test uses a steel test bit from a new cutter ring (Zare and Bruland 2013). The testing time is 1 min, which is equivalent to 20 revolutions. The AV and AVS tests are normally performed on 2–4 test pieces. An outline of the NTNU abrasion test is shown in Fig. 3c and the NTNU abrasion test apparatus in the Engineering Geology Laboratory of the Ferdowsi University of Mashhad (FUM) is shown in Fig. 3d.

In this study, a set of NTNU/SINTEF rock drillability tests were designed according to the procedures suggested by Dahl (2003). Based on such laboratory tests (with results shown in Table 6), the DRI, BWI, and CLI are determined for the tested rocks as follows.

5.1 Drilling Rate Index (DRI)

DRI is the most important input parameter of the NTNU model. The DRI was developed at the Engineering Geology Laboratory of the Norwegian Institute of Technology (NTNU) of the University of Trondheim in the 1960s for evaluating the drillability of rocks by percussive drilling (Selmer-Olsen and Lien 1960). The DRI is not a direct indicator of drilling rate in the field, but it is a relative measure of penetration rate and it is therefore not an absolute value of the drilling rate on the site. It may also be

Table 6 NTNU/SINTEF rock drillability parameters of the studied rocks

Rock code	S ₂₀ (%)	SJ (mm/10)	AV (mg)	AVS (mg)	DRI	BWI	CLI	VHNR (kg/mm ²)
R1	40.0	2.6	34	27.5	33	64	5.6	742
R2	50.8	2.7	52.5	45.5	45	49	4.6	810
R3	48.3	2.7	53.5	39	42	53	4.9	760
R4	52.6	4.1	9	25.5	48	34	6.9	700
R5	43.7	1.8	45.5	37	36	61	4.3	833
R6	31.6	2.4	4	8.5	25	54	8.6	768
R7	51.6	3.3	37	32	46	45	5.8	809
R8	51.5	3.0	44.5	24.5	45	48	6.2	826
R9	49.0	2.5	50	37.5	43	51	4.9	848
R10	40.7	3.5	21.5	23	36	54	6.7	785
R11	41.8	3.9	15.5	25.5	37	49	6.7	694
R12	49.3	3.9	24	28.5	45	44	6.4	814
R13	44.8	2.4	21	24	38	50	5.7	734
R14	28.0	2.1	10.5	9	21	77	7.9	741
R15	35.6	2.9	9	20.5	29	57	6.6	715
R16	33.4	3.3	5.5	5	28	52	11.8	718
R17	53.1	3.0	26.5	34.5	47	42	5.4	791
R18	33.8	4.8	7	20	30	53	8.0	752
R19	33.9	3.7	6	13.5	29	52	8.4	726
R20	32.5	3.0	4.5	17	26	54	7.1	754
R21	28.8	3.5	7.5	21.5	23	66	6.9	751
R22	44.0	3.4	19.5	30	39	48	6.0	780
R23	43.1	3.8	21	32	38	50	6.1	769
R24	53.3	4.5	14.5	15	50	35	8.7	770
R25	46.3	2.7	4.5	10.5	40	35	8.2	747
R26	55.6	3.2	34	33.5	50	41	5.6	800
R27	47.6	3.3	22	24	42	46	6.4	796
R28	27.7	4.3	5.5	21.5	23	62	7.5	700

viewed as a parameter for the maximum resistance of the rock to drilling (Yarali and Kahraman 2011). The DRI has been selected as the drillability parameter of intact rock. It is an indirect measure of the breaking work required, and an effective gauge of the rock breaking process under a cutter (Macias et al. 2014b). DRI is a combination of the S₂₀ that expresses the amount of energy required to crush the material and the Sievers J-value SJ that characterizes the depth a cutter can be thrust into the rock (Bruland 1998c). The diagram in Fig. 4a was used to assess the DRI based on S₂₀ and the SJ. From the diagram, the DRI of the tested rocks is computed (Table 6).

5.2 Bit Wear Index (BWI)

The BWI, which is used to estimate the wear rate of drill bits (Dahl et al. 2012), is assessed on the basis of the DRI and the AV (Selmer-Olsen and Lien 1960). Figure 4b is used to assess the BWI from the DRI and the AV. From the diagram, BWI of the tested rocks is computed (Table 6).

Due to the inefficiency of BWI for prediction of drill bit life in D&B tunneling, the wear parameter Vickers Hardness Number Rock (VHNR) is used instead of BWI in the updated NTNU prognosis models (Zare and Bruland 2013). However, it seems that the BWI can be an efficient index to predict drilling time and costs in D&B tunneling if the rock type blastability is taken into account.

The Vickers Hardness Number (VHN) is used as a measure of the hardness of each rock-forming mineral. The list of VHN for some rock-forming minerals is given by Bruland (1998d). Based on the list and mineral composition of the tested rock, the VHNR is calculated for each rock (Table 6), as follows:

$$\text{VHNR} = \sum \text{VHN}_i * (\% \text{mineral}_i / 100) \quad (5.1)$$

5.3 Cutter Life Index (CLI)

The development of the CLI (NTH 1983), which took place within 1980–1983, was based on the original NTH test

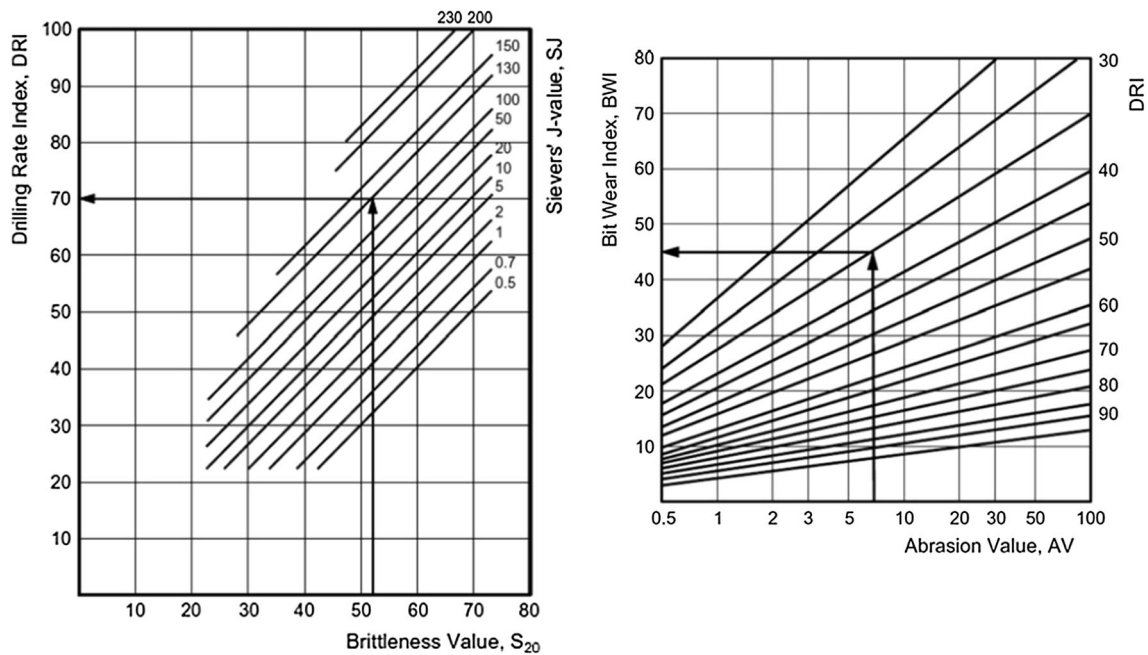


Fig. 4 Diagrams for assessment of **a** DRI and **b** BWI (Bruland 1998d)

method. The CLI has since the 1980s provided the possibility of estimating cutter life in connection with rock excavation by use of TBM (Dahl et al. 2012). Equation (5.2) is used to express the CLI during the boring process in hours for cutter disk rings of steel for the TBMs in terms of SJ and the AVS (Bruland 1998d):

$$\text{CLI} = 13.84 \left(\frac{\text{SJ}}{\text{AVS}} \right)^{0.3847} \quad (5.2)$$

6 Results and Discussion

The aim of this study is to evaluate the relationship between index properties and petrographical features of hard igneous rocks and NTNU/SINTEF drillability parameters. The feasibility of predicting NTNU/SINTEF drillability parameters based on index properties and petrographical features is discussed using a statistical analysis as follows.

6.1 Relationship Between Index Properties and NTNU/SINTEF Drillability Parameters

There are various studies in the literature that propose empirical correlations between mechanical properties and rock index properties such as dry density (ρ), porosity (ϕ), P-wave velocity (V_p), Schmidt rebound number (R_N), and point load strength index [$Is_{(50)}$] for different rock types (Deere and Miller 1966; Shorey et al. 1984; Katz et al.

2000; Lashkaripour 2002; Karakus et al. 2005; Shalabi et al. 2007; Yilmaz and Yuksek 2009; Yagiz 2011; Azimian et al. 2014; Liu et al. 2015; Aligholi et al. 2017b).

In this study, the relationships between index properties and NTNU/SINTEF rock drillability parameters of igneous rocks are investigated. For such a purpose, firstly the Pearson's correlation coefficient (R) between the above-mentioned engineering properties was inquired using the following equation:

$$R_{xy} = \frac{\text{cov}(x, y)}{s_x s_y} \quad (6.1)$$

where, to find the correlation between the variables, covariance is divided by the standard deviation values for each regression model (Table 7).

As shown in Table 7, there are negative correlation coefficients between density, initial wave velocity, and $Is_{(50)}$ on one hand and S_{20} , AV, AVS, and DRI of the studied rocks, on the other hand. Also, there are positive correlation coefficients between such index properties and BWI and CLI. Therefore, the increase in engineering quality of the studied rocks, which is represented in their index properties such as density, the initial wave velocity and $Is_{(50)}$, results in a decrease in their S_{20} and DRI and increase in their BWI. Based on the results of this study, which is conducted on a wide range of unweathered igneous rocks with no alteration, the acidic rocks compared to the intermediate to basic rocks have a lower density, P-wave velocity, and strength. As a result, the BWI, which is highly affected by DRI (Fig. 4b), is lower in acidic rocks

Table 7 Pearson's correlation coefficient between index properties and NTNU/SINTEF rock drillability parameters

	S_{20} (%)	SJ (mm/10)	AV (mg)	AVS (mg)	DRI	BWI	CLI
ρ (gr/cm ³)	-0.72	0.16	-0.54	-0.48	-0.70	0.41	0.39
ϕ (%)	0.46	0.07	0.17	0.13	0.48	-0.38	-0.07
V_p (m/s)	-0.78	0.16	-0.67	-0.63	-0.76	0.40	0.55
R_N	-0.21	-0.11	-0.01	0.08	-0.22	0.11	-0.05
$Is_{(50)}$ (MPa)	-0.70	0.01	-0.66	-0.60	-0.70	0.34	0.46

compared to the basic ones. Furthermore, because these acidic igneous rocks contain higher amounts of quartz, they have a higher AV and AVS and, consequently, a lower CLI compared to the basic rocks.

Abrasion in TBM cutters may be critical in terms of project duration and costs (Espallargas et al. 2015). Large investments and high geological risk are involved using TBMs. Besides, disk cutter consumption has a great influence on performance and cost, especially in hard rock conditions (Macias et al. 2016). Thus, it seems that based on NTNU/SINTEF indices, TBM tunneling in hard basic igneous rocks with lower abrasion potential involves fewer problems compared to the acidic rocks. Moreover, it is economic and fast compared to D&B tunneling. However, for the acidic igneous rocks, which have a considerably higher abrasion potential and lower engineering quality compared to basic rocks regardless of the time required, D&B tunneling involves lower costs. However, selection of the cost effective excavation method for a tunnel is a function of tunnel cross-section area, rock conditions, tunnel length, availability of skilled labor and proper equipment, and project schedule (Zare et al. 2016).

Moreover, the correlation between index properties and drillability parameters for the rocks studied in the present work was analyzed using the univariate regression analysis. Based on the obtained results, there are mostly linear relations between the index properties and drillability parameters of the igneous rocks. The correlation coefficient (R^2) obtained from the univariate regression of these properties are shown in Table 8. For some cases, the univariate regression using the nonlinear functions such as exponential, logarithmic, and power are more accurate. As shown in Fig. 5, using power function compared to the linear function in univariate regression provides a higher R^2 between porosity and S_{20} . As presented in Tables 7 and

8, among the index properties of the rocks studied in this work, P-wave velocity has the optimum performance in prediction of rock drillability (Fig. 6). According to Fig. 6b, applying exponential function provides a better result for prediction of AV using P-wave velocity, probably because of the quartz content of the studied rocks.

As S_{20} and point load strength are two different test methods for determining strength properties of rock, a high correlation between S_{20} and $Is_{(50)}$ might be expected. On the contrary, based on the results of this study, these two tests show a relatively poor relation (Fig. 7). This behavior might be explained by the fact that S_{20} is performed by applying repeated impacts on the sample material, which causes crushing of the sample material while $Is_{(50)}$ is performed by applying a load on the sample at a constant relatively slow rate until failure occurs (Dahl et al. 2012).

Based on the results shown in Table 8, there is no statistically significant relation between Schmidt rebound number (R_N) and drillability indices of the studied rocks. However, Aligholi et al. (2017b) reported that rocks with different rebound values indicate different physical and mechanical properties. Thus, rock hardness classification is a considered a prerequisite in the mechanical assessment of rock properties in terms of rock index properties. These authors showed that by classifying rocks based on Schmidt rebound number, prediction of strength and brittleness in igneous rocks using their density, porosity, rebound number, and P-wave velocity provide more valid results.

Because rock powder is used in AV and AVS tests, no correlation is expected between the results of these tests and rock porosity. Moreover, because the SJ of the studied rocks are generally low (Table 6), no relation was found between SJ and rock index properties. It should be noted that a low SJ-Value is indicating a high surface hardness and resistance to penetration (Dahl et al. 2012).

Table 8 Correlation coefficient (R^2) from simple linear regression analysis between index properties and NTNU/SINTEF rock drillability parameters

	S_{20} (%)	SJ (mm/10)	AV (mg)	AVS (mg)	DRI	BWI	CLI
ρ (gr/cm ³)	0.51	0.03	0.29	0.23	0.49	0.16	0.15
ϕ (%)	0.21	0.01	0.03	0.02	0.23	0.15	0.01
V_p (m/s)	0.61	0.03	0.45	0.40	0.58	0.16	0.30
R_N	0.04	0.01	0.00	0.01	0.05	0.01	0.00
$Is_{(50)}$ (MPa)	0.49	0.00	0.43	0.36	0.49	0.11	0.21

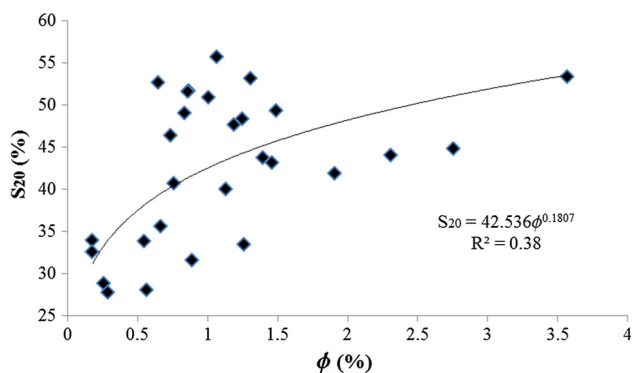


Fig. 5 Correlations between S_{20} and porosity using power function

The empirical relationships between mechanical properties of rocks and index tests are a common procedure in engineering geology for reducing both time and costs. Typically, these relations are different for various parts of the world, depending on the regional tectonic, rock formation conditions, and environmental conditions such as temperature and hydrothermal solutions. These factors may result in many changes in hardness, density, porosity, fractures and discontinuities, weathering and alteration, mineralogical composition, and textural and microstructure of the rocks which affect the mechanical properties of the rocks. Thus, merely using a simple test such as Schmidt hammer test or P-wave velocity may not provide an accurate and practical equation for estimation of rock

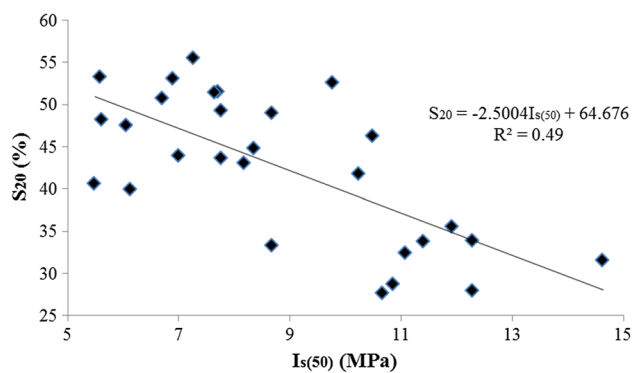


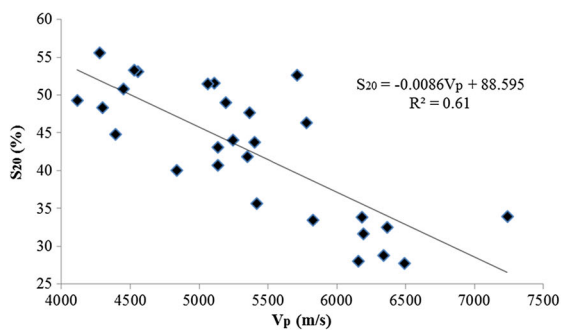
Fig. 7 Relationship between S_{20} and $I_{s(50)}$

properties in different parts of the world. In this regard, estimation of mechanical properties and drillability of rocks using multiple index parameters provides more valid equations.

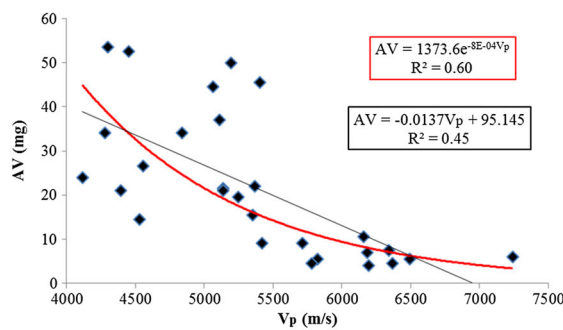
In order to describe the relationships between multiple index properties and drillability parameters of the tested rocks, a multiple regression model with a 95% confidence level by considering linear functions was applied:

$$Y = \beta_0 + \beta_1x_1 + \beta_2x_2 + \dots + \beta_nx_n \tag{6.2}$$

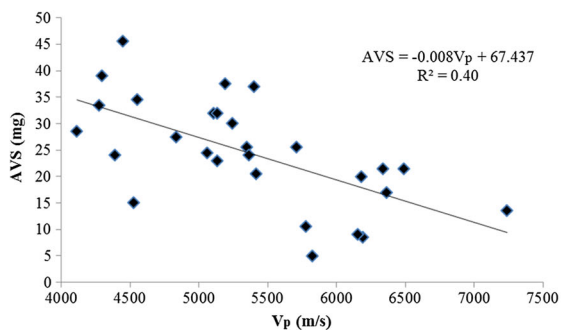
where Y is the dependent variable, β_0 is a constant value, x_1 to x_n are the independent variables, and β_1 to β_n are partial regression coefficients for x_1 to x_n , respectively. The results of the regression analyses are given in Table 9. To examine the validity of the statistical models, the measured



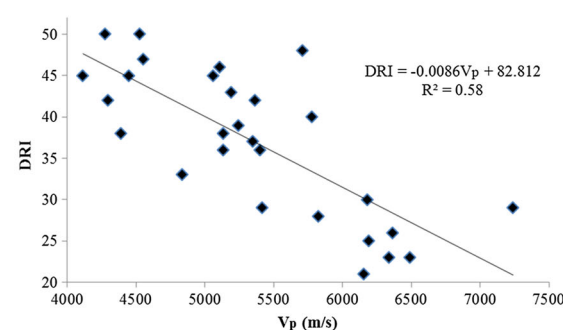
(a)



(b)



(c)



(d)

Fig. 6 P-wave velocity versus some NTNU/SINTEF rock drillability parameters: **a** S_{20} ; **b** AV; **c** AVS; and **d** DRI

Table 9 Summary of the multiple regression models between index properties and NTNU/SINTEF rock drillability parameters as well as some statistical parameters for examining the validity of the developed models

Dependent variable	S ₂₀ (%)	SJ (mm/10)	AV (mg)	AVS (mg)	DRI	BWI	CLI
Constant	120.47	1.27	128.98	55.53	112.43	33.11	2.31
<i>Regression coefficient of independent variables</i>							
ρ (gr/cm ³)	-16.944	1.075	-8.303	1.329	-15.667	11.150	-0.324
ϕ (%)	-0.580	0.069	-7.901	-3.262	-0.314	-4.033	0.536
V _p (m/s)	-0.006	0.001	-0.014	-0.011	-0.005	0.004	0.002
R _N	0.090	-0.052	0.244	0.556	0.026	-0.409	-0.084
Is ₍₅₀₎ (MPa)	-0.347	-0.199	-1.918	-0.280	-0.627	-0.776	-0.070
<i>Performance index</i>							
R ²	0.66	0.20	0.61	0.58	0.63	0.23	0.46
RMSE	5.57	0.72	11.20	7.24	5.94	9.31	1.27
P value	0.000	0.393	0.001	0.001	0.000	0.289	0.014

drillability properties values based on laboratory tests were plotted versus the predicted values from these models (Fig. 8). A comparison between results shown in Tables 8 and 9 clearly shows that the multiple regression model provides more accurate results compared to the univariate regression model. In general, the conducted statistical analysis does not provide reliable equations and correlations between the index properties and drillability properties of the igneous rocks. However, based on the conducted studies, it seems that making a classification for igneous rocks on the basis of their petrography properties may result in more reliable and accurate prediction of drillability properties in these rocks using their index properties.

6.2 Relationship Between Petrographic Features and NTNU/SINTEF Drillability Parameters

To study the relationship between petrographic and drillability properties of the studied rock specimens, first, the Pearson's correlation coefficient was assessed between these parameters (Table 10). Based on the results of this study, among the petrographic features, mineralogical indices, and grain size descriptors indicate a higher correlation with drillability properties of the studied igneous rocks. As shown in Table 10, no individual statistically significant relation is identified between the drillability properties and grain shape descriptors and texture coefficients. The low correlation between the studied textural indices [interlocking (*g*) and grain size homogeneity (*t*)] are probably because the effect of particle size and rock mineralogical composition was not considered in these indices.

As mentioned earlier, because SJ is generally low in the studied rocks, no significant equation was found between this parameter and petrography properties. Based on the data shown in Table 10, a positive correlation is

detected between the S₂₀ and DRI, and grain size descriptors of the studied rocks. Furthermore, positive correlation values were identified between S₂₀ and DRI, and saturation index (IS), feldspar index (IF), and Vicker's hardness number of rock (VHNR) and a negative correlation with coloration index (IC). Based on these observations it can be deduced that the fine-grained and basic igneous rocks are more resistant compared to the acidic and coarse-grained rocks and possess higher engineering quality. In addition, BWI, which is mainly a function of DRI rather than AV, indicates a higher value in fine-grained and basic igneous rocks. However, considering the effect of AV, no individual significant relation is found between BWI and petrographic features of igneous rocks. But, since the fine-grained rocks are mainly intermediate to basic, their low quartz content and, consequently, lower AV results in a greater CLI in these rocks. It is noteworthy that there is a negative correlation between CLI and mineralogical indices (IS, IF, and VHNR) and a positive correlation between CLI and IC (Table 10). Accordingly, as mentioned earlier, CLI in igneous rocks with high quartz content is shorter compared to that of intermediate to basic igneous rocks.

Because rock powder is used to carry out NTNU/SINTEF abrasion (AV and AVS) tests, it is not possible to study the effect of textural features such as grain size and shape and textural indices on abrasion potential of the rocks. However, the NTNU/SINTEF drillability indices (DRI, BWI, and CLI) are combinational and might be estimated using different rock properties such as abrasion, brittleness, and hardness. In this method, the designed abrasion tests are on the basis of the mineralogical composition of rocks. The combination of the values obtained from these tests with S₂₀ and SJ provides the valid BWI and CLI indices for tunneling trend evaluation using the D&B method or the mechanized excavation using TBM.

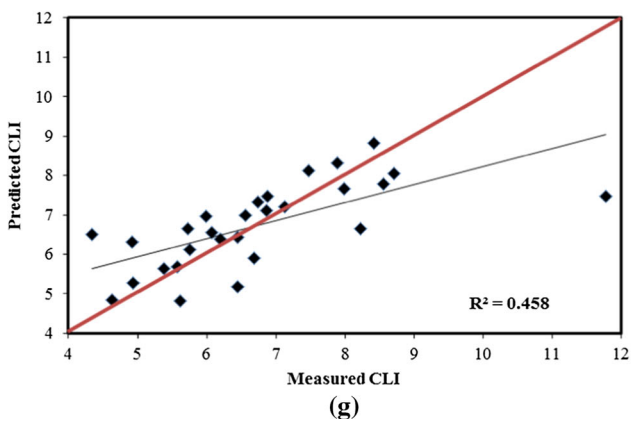
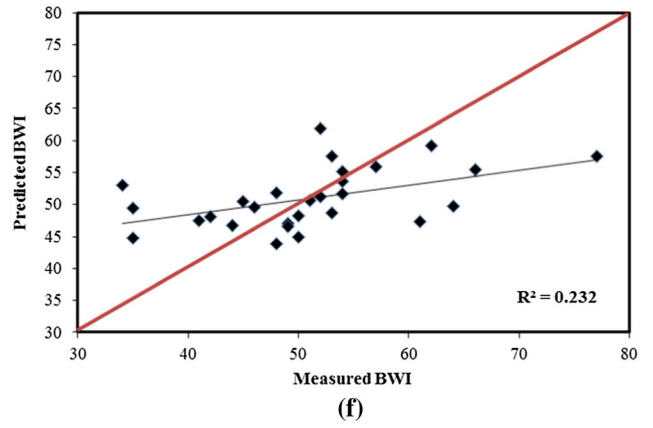
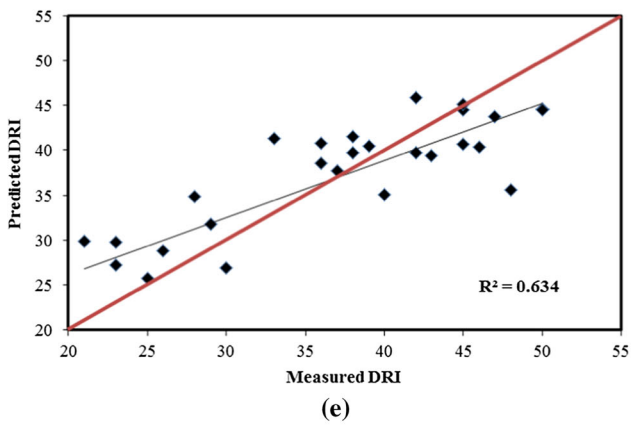
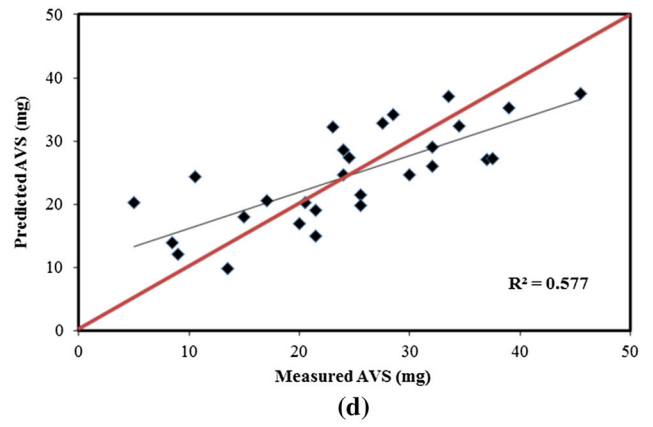
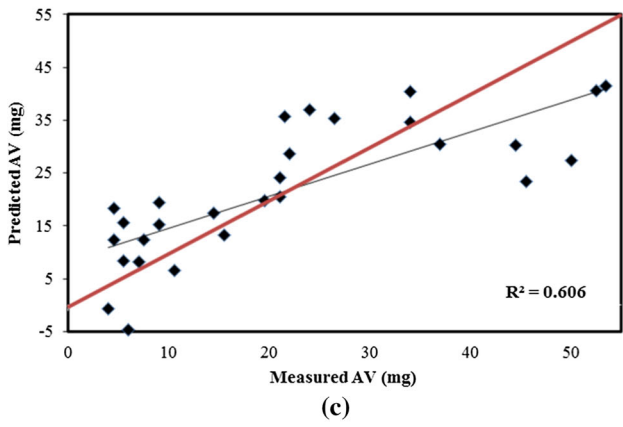
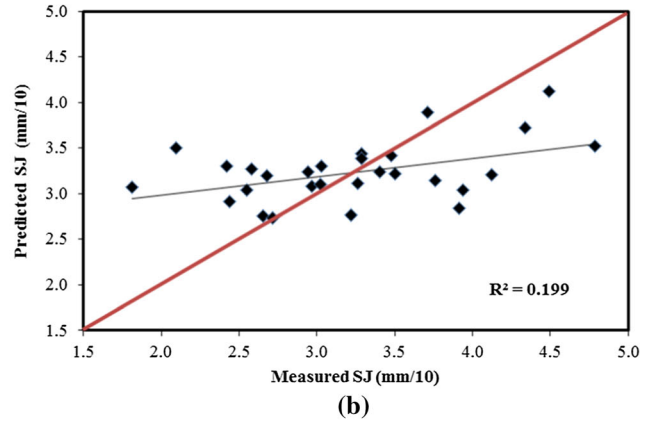
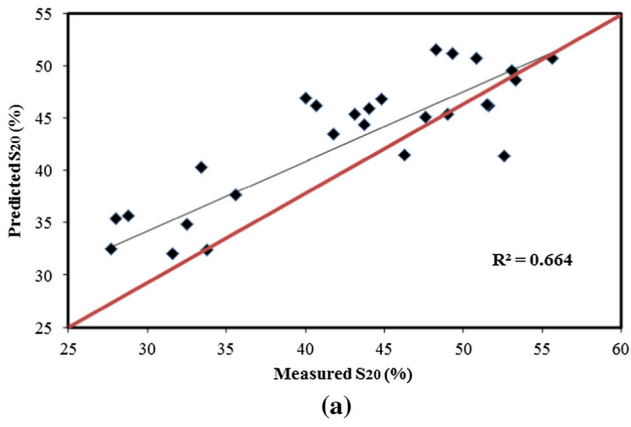


Fig. 8 Graphs of the predicted drillability parameters from index properties versus the measured drillability parameters: S_{20} (a), SJ (b), AV (c), AVS (d), DRI (e), BWI (f), and CLI (g)

As shown in Table 10, among the studied mineralogical indices, IS (which is calculated based on quartz to the sum of quartz and feldspar contents of rock) has the maximum correlation with both AV and AVS tests. The AV test, which is performed on a piece of tungsten carbide and is used in drilling bit life estimation in D&B tunneling, is highly correlated with the IS. In this connection, NTNU/SINTEF researchers have found many shortcomings in BWI and are replacing it with VHNR. However, the mineralogical indices proposed in the present work, particularly IS, indicate a much higher correlation compared to VHNR with outputs of both AV and AVS tests. Thus, saturation index is presented as a new parameter for estimation of bit wear in igneous rocks.

The relations between saturation index and AV as well as AVS for the studied rocks are presented in Fig. 9. As shown in Fig. 9a, there is a high correlation between saturation index and AV results. As noted by Dahl et al. (2012), the low quartz content gives AV and AVS of the same magnitude, while its high content leads to an AV higher than the AVS. A comparison between Fig. 9a, b reveals that an increase in saturation index (as a function of

quartz content in the rock) leads to a higher AV compared to AVS. Thus, the exponential function provides a better correlation between saturation index and AV. An explanation for this observation is might be the high hardness of quartz, which enables quartz to cause a significantly higher degree of abrasion on tungsten carbide than other minerals are able to do (Dahl et al. 2012). In other words, since tungsten carbide is harder than cutter ring steel, it is abraded only with very hard minerals such as quartz and is resistant to other minerals. Although cutter steel is abraded with minerals with lower hardness, this abrasion is not directly related to the hardness level of minerals used in rock powder preparation. To understand this behavior, the correlation between VHNR (which is an index of hardness level and abrasiveness of rock minerals) and AVS was analyzed (Fig. 10), where no explicit correlation was found between VHNR and AVS. An explanation for this result might be the difference in soft minerals content in the mineralogical composition of the studied rocks. To illustrate this issue, some rock samples with almost the same AV are shown in Table 11. Moreover, the soft minerals content of this rocks (biotite% + muscovite% + chlorite%) are also shown in this table. Based on the data shown in this table, it is clearly seen that an increase in soft minerals content leads to a severe declination in AVS while having the same AV. In other words, the soft minerals lead to a decrease in rock (powder) abrasion potential against

Table 10 Pearson's correlation coefficient between petrographic features and NTNU/SINTEF rock drillability parameters

	S_{20} (%)	SJ (mm/10)	AV (mg)	AVS (mg)	DRI	BWI	CLI
<i>Size descriptors</i>							
Area	0.54	0.22	–	–	0.57	–0.40	–0.24
Perimeter (mm)	0.57	0.21	–	–	0.59	–0.36	–0.36
Size (mm)	0.64	0.19	–	–	0.66	–0.40	–0.42
Min of Feret's (mm)	0.64	0.20	–	–	0.66	–0.40	–0.41
<i>Shape descriptors</i>							
Max of Feret's (mm)	0.61	0.19	–	–	0.63	–0.38	–0.41
Elongation	–0.15	–0.17	–	–	–0.16	0.05	0.07
Orientionation (°)	0.19	–0.03	–	–	0.18	–0.42	0.10
Eccentricity	–0.18	0.06	–	–	–0.17	0.03	0.17
Compactness	–0.07	–0.20	–	–	–0.09	0.00	0.08
Rectangularity	–0.37	0.22	–	–	–0.34	0.31	0.23
Solidity	0.50	–0.09	–	–	0.49	–0.42	–0.31
Convexity	–0.15	–0.23	–	–	–0.17	0.09	0.09
<i>Texture coefficients</i>							
<i>g</i>	–0.15	–0.20	–	–	–0.17	0.25	0.01
<i>t</i>	0.28	0.13	–	–	0.29	–0.38	–0.01
<i>Mineralogical indices</i>							
IS	0.65	–0.39	0.90	0.70	0.61	–0.10	–0.67
IF	0.66	–0.14	0.76	0.62	0.65	–0.26	–0.53
IC	–0.71	0.26	–0.72	–0.60	–0.68	0.26	0.54
VHNR	0.54	–0.33	0.71	0.55	0.51	–0.16	–0.53

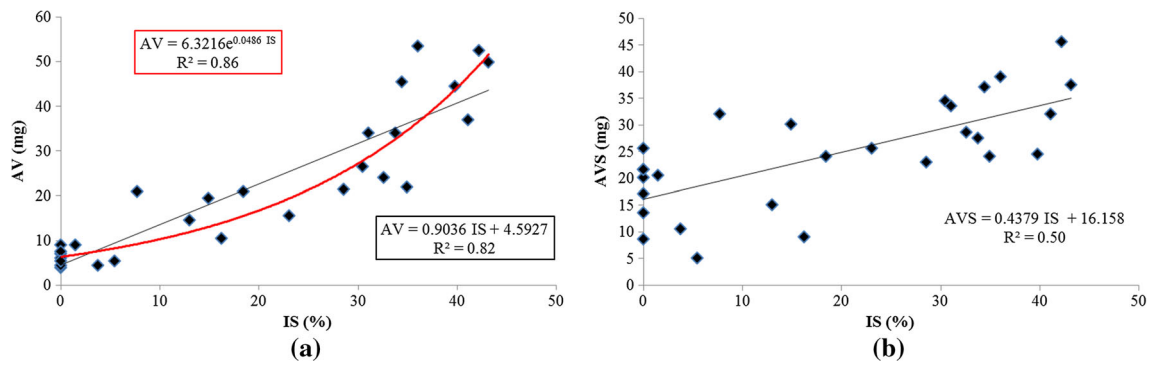


Fig. 9 Correlations between saturation index (IS) and: **a** AV and **b** AVS

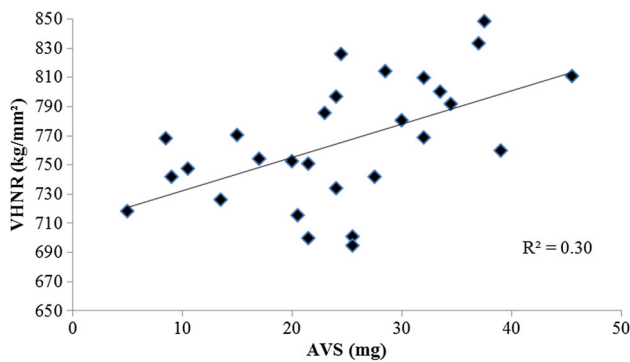


Fig. 10 Relationship between Vickers Hardness Number Rock (VHNR) and AVS

cutter ring steel; the high soft mineral content, the more severe this declination. In contrast, rock (powder) abrasion potential against tungsten carbide is independent of its soft minerals content and is a function of highly abrasive minerals such as quartz.

In addition, using the multiple linear regression modeling, two equations were developed between the mineralogical indices (IS, IF, and IC) and AV and AVS tests, shown in Table 12a. Figure 11 shows the AV and AVS predicted using multiple linear regression with their measured values. As shown in Table 12a, no significant correlation increase is seen compared to univariate linear regression between IS and both AV and AVS (Fig. 9). Accordingly, as mentioned earlier, AV in igneous rocks is

Table 11 AV, AVS, and soft minerals content from some studied rocks with the same AV

Rock code	AV (mg)	AVS (mg)	Soft minerals (%)
R10	21.5	23	7
R13	21	24	9
R22	19.5	30	1
R23	21	32	1
R27	22	24	8

highly controlled by their quartz content. For AVS test, the effect of each mineral (particularly the soft ones) in mineralogical composition of rock and rock powder requires a further investigation.

To check whether abrasiveness potential of the studied rocks are mainly controlled by the IS as well as find the best mineralogical indices in order to predicting AV and AVS, the multiple linear regression models using the forward stepwise method are also applied (Table 12b). The results prove that among the studied mineralogical indices, IS is the most proper one to predict both AV and AVS.

Table 12 (a) Summary of the multiple regression models between mineralogical indices and NTNU abrasion tests and (b) Summary of the stepwise multiple regression models

Dependent variable	AV (mg)	AVS (mg)
A		
Constant	-4.178	15.055
<i>Regression coefficient of independent variables</i>		
IS (%)	0.825	0.341
IF (%)	0.188	0.085
Ic (%)	0.198	0.013
<i>Performance index</i>		
R ²	0.84	0.52
RMSE	6.79	7.40
F-statistic	43.0	8.6
P value	0.000	0.000
B		
Constant	4.593	16.158
<i>Regression coefficient of the selected independent variable</i>		
IS (%)	0.904	0.438
<i>Performance index</i>		
R ²	0.82	0.50
RMSE	7.06	7.27
F-statistic	115.2	25.6
P value	0.000	0.000

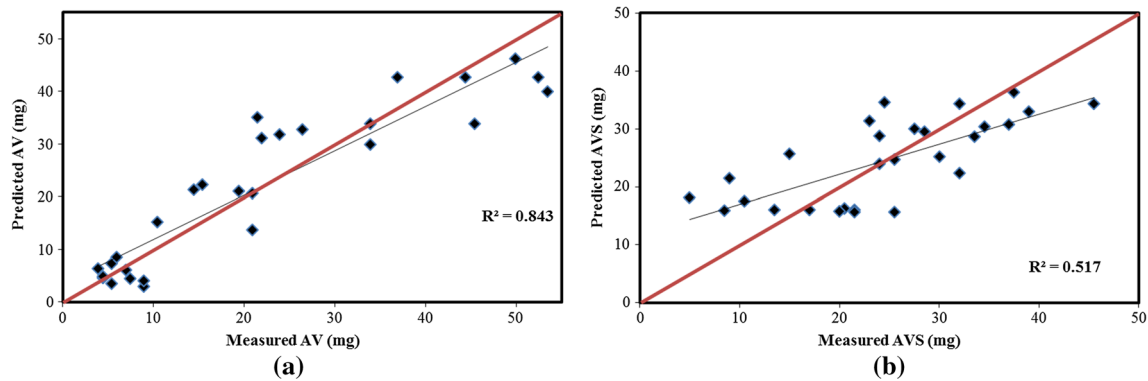


Fig. 11 Correlations between measured AV (a) and AVS (b) and their corresponding predicted values from mineralogical indices

To further investigate the effect of quartz content of igneous rocks on their abrasion potential, a comparison was made between the data obtained from the present study and the one conducted by Bruland (1998e), which had been conducted on a variety of rocks with different petrology. Bruland (1998e) proposed equations between DRI and BWI as well as SJ and CLI in terms of quartz content of the studied rocks. As mentioned earlier, BWI is estimated using DRI and AV, while CLI is predicted using SJ and AVS. Thus, when studying the relationship between DRI and BWI or SJ and CLI with quartz content, somehow the effect of quartz content on AV and AVS as well as a feasibility study of predicting BWI and CLI with quartz content rather than performing abrasion test is evaluated. Bruland (1998e) concluded that by classification of quartz content of rocks (Table 13), BWI and CLI would provide remarkably more accurate results in terms of DRI and SJ, respectively. Nevertheless, as the table also shows, the equations proposed for determination of BWI are of higher correlation, meaning that AV compared to AVS indicates a higher correlation with quartz content.

The relations between DRI and BWI and those between SJ and CLI for the studied igneous rocks are shown in Fig. 12a, b. The equations proposed by Bruland (1998e) were evaluated in the present work with quartz content of the rocks (Fig. 13). In this regard, considering the classification systems such as that of Streckeisen (1976) proposed for igneous rocks, a more accurate classification was proposed for the igneous rocks (Table 14). According to this classification, the relationship between BWI and DRI and quartz content of igneous rocks was studied further (Fig. 14a). As shown in Fig. 14b, the classification proposed for prediction of BWI in igneous rocks based on DRI and the equivalent quartz content was highly successful. Therefore, it can be used to decline the time and costs involved in AV test to measure BWI. However, as shown in Fig. 15, predicting CLI with quartz content for igneous rocks rather than

Table 13 Relationships between quartz content and: (a) BWI and DRI and (b) CLI and SJ (Bruland 1998e)

Quartz content	Equation	R^2
A		
0–10%	$BWI = 0.007DRI^2 - 1.39DRI + 78$	0.97
11–20%	$BWI = 0.009DRI^2 - 1.77DRI + 94$	0.92
21–40%	$BWI = 0.013DRI^2 - 2.32DRI + 121$	0.88
41–70%	$BWI = 0.014DRI^2 - 2.58DRI + 133$	0.75
71–100%	$BWI = 0.017DRI^2 - 2.99DRI + 149$	0.67
B		
0–5%	$CLI = 4.2346SJ^{0.6234}$	0.69
6–10%	$CLI = 4.7835SJ^{0.5366}$	0.53
11–20%	$CLI = 3.7432SJ^{0.5399}$	0.77
21–40%	$CLI = 3.242SJ^{0.5165}$	0.81
41–100%	$CLI = 3.7428SJ^{0.4317}$	0.85

performing AVS test is efficient only for the acidic rocks with quartz content higher than 20%. Therefore, soft minerals also play a key role in AVS prediction; the lower the quartz content in the rock, the higher the effect of soft minerals (Fig. 15).

Most problems in mining and geology involve complex and interacting forces, which are impossible to isolate and study separately (Davis 1973). Some of the rock properties which highly affect the progress rate and the equipment wear in mining, tunneling, and underground construction are mineralogy, texture, grain shape, grain binding, and grain size (Dahl et al. 2007). Hence, for a reliable and robust prediction of rock drillability properties, a reasonable combination of some petrographic features is required.

In order to describe the relationships between the petrographic features and drillability properties of the tested rocks, multiple regression model was applied by considering the linear functions. The results of the regression analyses are given in Table 15. To check the validation of

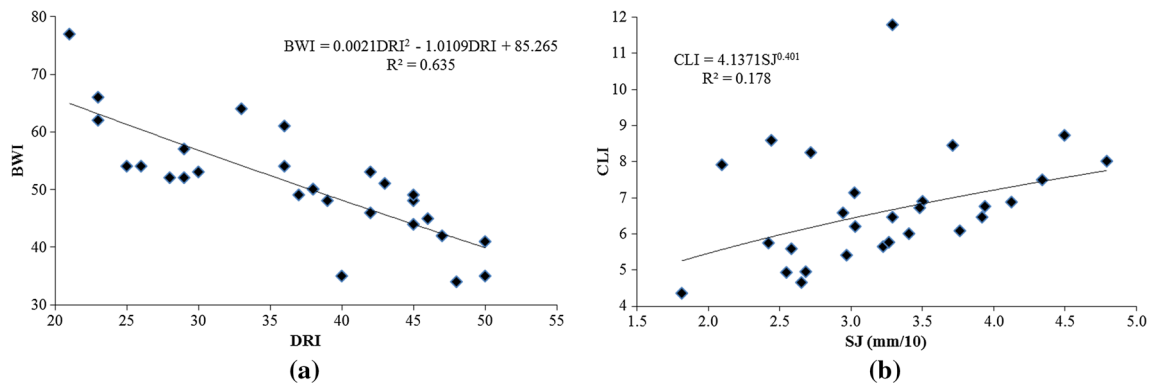


Fig. 12 a BWI with DRI and b CLI with SJ

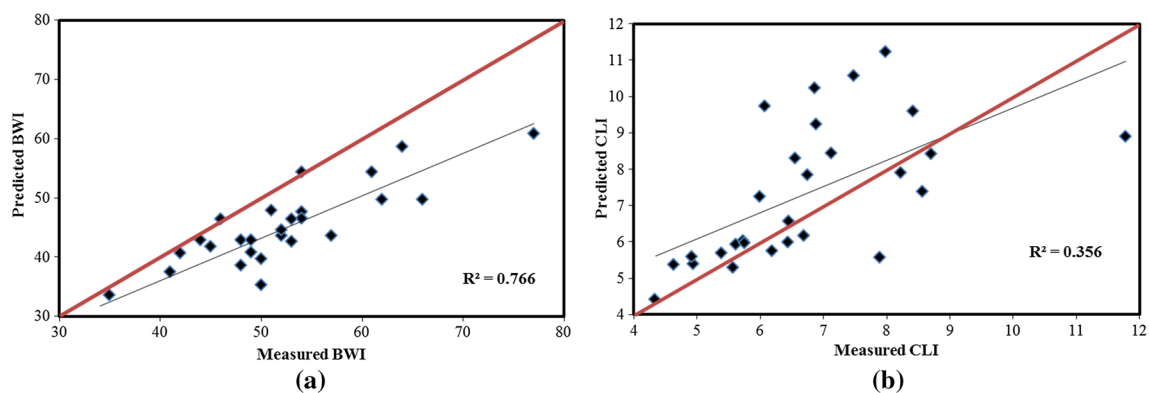


Fig. 13 Graphs of the predicted BWI versus the measured BWI (a) and the predicted CLI versus the measured CLI (b) based on Bruland (1998e) equations

Table 14 Proposed relationships between quartz content and BWI and DRI

Quartz content (%)	Equation	R^2
<5	$BWI = 0.032DRI^2 - 3.47DRI + 125.3$	0.904
6–20	$BWI = 0.016DRI^2 - 2.55DRI + 123.6$	0.996
>20	$BWI = 0.015DRI^2 - 2.55DRI + 130.8$	0.866

the statistical models, the values of the measured drillability properties are plotted with those predicted using these models (Fig. 16).

Based on the results shown in Table 15, the prognosis models for S_{20} , DRI, and BWI in terms of petrographic features offer a high correlation and a low error. The results also showed that the multiple linear regression of the petrographic features provides more valid and reliable results for drillability properties of the studied igneous rocks that in many cases can obviate the need for time-consuming expensive tests. Figure 16 also

clearly shows that, except the prognosis model for SJ (Fig. 16b) and CLI (Fig. 16e), the points are close to the regression line, implying the validity of the proposed models. In this connection, it seems that the crystal grid network of the constituting minerals of the studied rocks and the bond energy among the atoms of their minerals is a controlling factor, without which it is not possible to provide an accurate estimation of resistance against the penetration of drilling bits to rocks. The CLI index, on the other hand, is estimated using the SJ and AVS parameters. Thus, the factors causing the inaccuracy of the estimated SJ are also effective in this parameter. Furthermore, as shown in Fig. 11 and Table 12, it is clear that use of mineralogical indices of the studied rocks is not accurate enough in AVS estimation. Thus, it seems that to laboratory tests are necessary for reliable estimation of CLI. However, it is possible to apply petrography analyses for an early estimation, classification of rock masses, and initial planning for laboratory tests for CLI prediction in TBM projects.

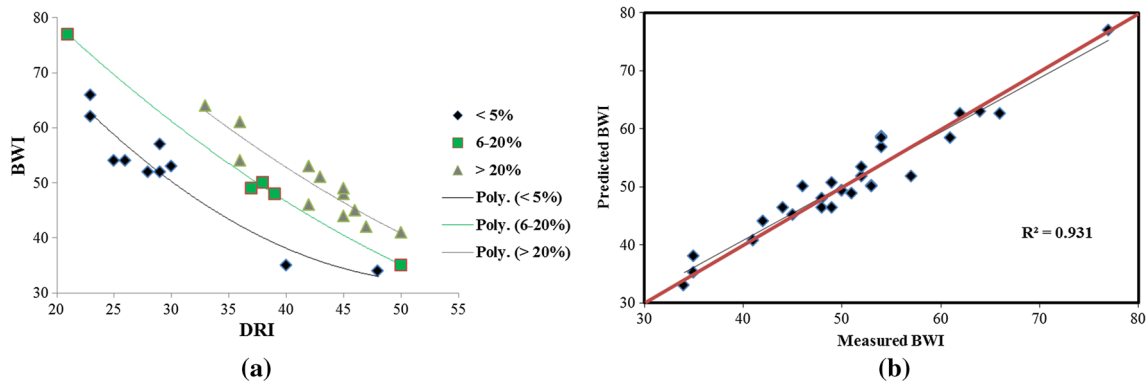


Fig. 14 **a** BWI versus DRI for each proposed quartz content class and **b** the measured BWI versus the predicted BWI based on the proposed equations

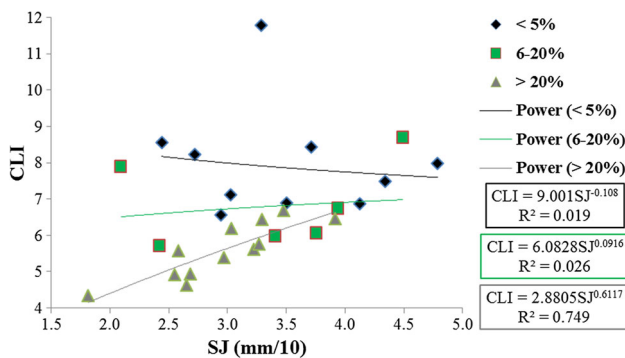


Fig. 15 CLI versus SJ for each proposed quartz content class

7 Conclusion

In this research, the drillability potential was studied for a wide range of hard igneous rocks without any detectable cracks, fractures, weathering, and alteration using the drillability parameters proposed by NTNU/SINTEF. The extracted results from the laboratory tests and petrographical studies showed that AV compared to AVS is highly correlated with saturation index (IS), which is a mineralogical index estimated based on the ratio of quartz to quartz and feldspar. On the other hand, results showed that AVS criterion is not strongly correlated with rock quartz content and other studied mineralogical indices such as Feldspathic index (IF), coloration index (IC), and Vickers Hardness Number Rock (VHNR). Thus, it may be concluded that because tungsten carbide (as the test piece used in AV test) is harder than the cutter ring steel (the test piece used in AVS test), it is abraded only with very hard minerals such as quartz. In comparison, the cutter ring steel would be more susceptible to wear against softer minerals. In addition, AVS is affected by

not only the hardness of the constituting minerals of the rock but also the factors related to the mineralogical composition of the rock (powder). For example, minerals such as mica or clay minerals generated by the alteration of feldspars might considerably affect AVS. According to this study, this behavior is more notable in igneous rocks with quartz content <20%.

Based on the results of this investigation, the acidic igneous rocks indicate a lower strength and density and a higher S_{20} compared to those for basic rocks. Overall, the SJ parameter was notably low for hard igneous rocks and it seems that it is controlled by the crystal grid network of the constituting minerals of the rocks and the bond energy of the constituting atoms of the minerals, in addition to the petrographical properties. As a result, DRI, which is estimated based on S_{20} and SJ, is higher in acidic igneous rocks. In addition, the BWI, as a parameter estimated using DRI and AV (with DRI having a stronger control over it compared to AV), is generally lower in acidic igneous rocks. Thus, D&B tunneling in these rocks is more convenient and involves lower costs compared to basic rocks. However, CLI in these rocks is lower compared to basic rocks. Hence, it seems that, based on the NTNU/SINTEF drillability parameters, tunneling in hard intermediate to basic igneous rocks with a lower abrasion potential involves less complexities using TBM tunneling and is faster and more economic compared to D&B tunneling.

In this study, a semiautomatic procedure was proposed for the analysis of microscopic images of the studied rocks. The steps of this procedure are: (1) generation of representative images using a digital camera mounted on a microscope; (2) image preprocessing and segmentation; (3) extraction of petrographical features; and (4) multiple linear regression analysis for prediction of rock

Table 15 Summary of the multiple regression models between petrographic features and NTNU/SINTEF rock drillability parameters

Dependent variable	S ₂₀ (%)	SJ (mm/10)	DRI	BWI	CLI
Constant	435.37	43.48	462.48	-498.80	-81.21
<i>Regression coefficient of independent variables</i>					
Area (mm ²)	0.860	2.264	5.353	-13.72	3.126
Perimeter (mm)	-3.352	-1.012	-5.507	10.34	-1.360
Size (mm)	128.67	5.226	112.65	-201.37	-27.61
Min of Feret's (mm)	3.824	4.292	30.84	-62.61	94.19
Max of Feret's (mm)	-66.37	-1.997	-65.80	124.78	-33.46
Elongation	-69.60	-3.155	-69.72	63.18	26.24
Orienetation (°)	0.740	-0.040	0.673	-1.163	-0.058
Eccentricity	6.204	-0.191	5.766	-8.449	-0.206
Compactness	-97.77	-30.50	-139.54	100.24	15.18
Rectangularity	-98.83	-9.805	-109.51	140.51	11.95
Solidity	-145.85	-45.44	-181.77	260.12	28.68
Convexity	-73.76	26.65	-44.34	137.58	8.011
<i>g</i>	-1.189	-0.247	-1.506	1.760	0.180
<i>t</i>	1.200	-1.575	-3.587	17.11	-19.70
IS (%)	0.071	-0.036	0.025	0.202	-0.059
IF (%)	0.007	0.015	0.034	-0.043	0.014
IC (%)	-0.226	0.027	-0.184	0.118	0.028
<i>Performance index</i>					
R ²	0.96	0.76	0.95	0.86	0.71
RMSE	2.89	0.58	3.33	5.99	1.38
<i>P</i> value	0.000	0.155	0.000	0.025	0.286

engineering properties. The results derived from the multiple linear regression prove the power and efficiency of the petrographical procedure proposed for prediction of drillability properties of igneous rocks. In this regard, the selected textural properties and mineralogical indices were also found as highly effective parameters; as in the case of implementing a well-organized method, these properties might be useful in the accurate prediction of several rock engineering properties and obviate the use of the time-consuming expensive testing procedure.

Moreover, the relationship between rock index properties such as density, porosity, P-wave velocity, Schmidt hammer rebound hardness number (R_N), and $I_{s(50)}$ and drillability parameters proposed by NTNU/SINTEF was analyzed using the Pearson's correlation (R) coefficient, univariate linear regression, and multiple linear regression. Based on the conducted statistical analyses, it was found that there are some statistically significant relationships between density, P-wave velocity, and $I_{s(50)}$ and drillability parameters of the

igneous rocks; with P-wave velocity having the highest correlation with drillability parameters. Furthermore, the multiple regression models, compared to univariate regressions, indicate a higher accuracy and, except for SJ and BWI, provide acceptable predictions for the drillability indices of NTNU/SINTEF. Nevertheless, except for AVS for which the same results were achieved, the accuracy of the multiple regression statistical models developed based on the index parameters is drastically lower than those developed using the petrographical characteristics.

Based on the results obtained from this study, further studies are required for a better understanding of the effect of soft minerals such as mica or the secondary minerals generated by alteration such as clay minerals and chlorite in the mineralogical composition of rock on AVS. It is also suggested performing further investigations on the effect of structural characteristics of rocks at a molecular scale on SJ parameter. The results of such investigations might be valuable in understating the pen-

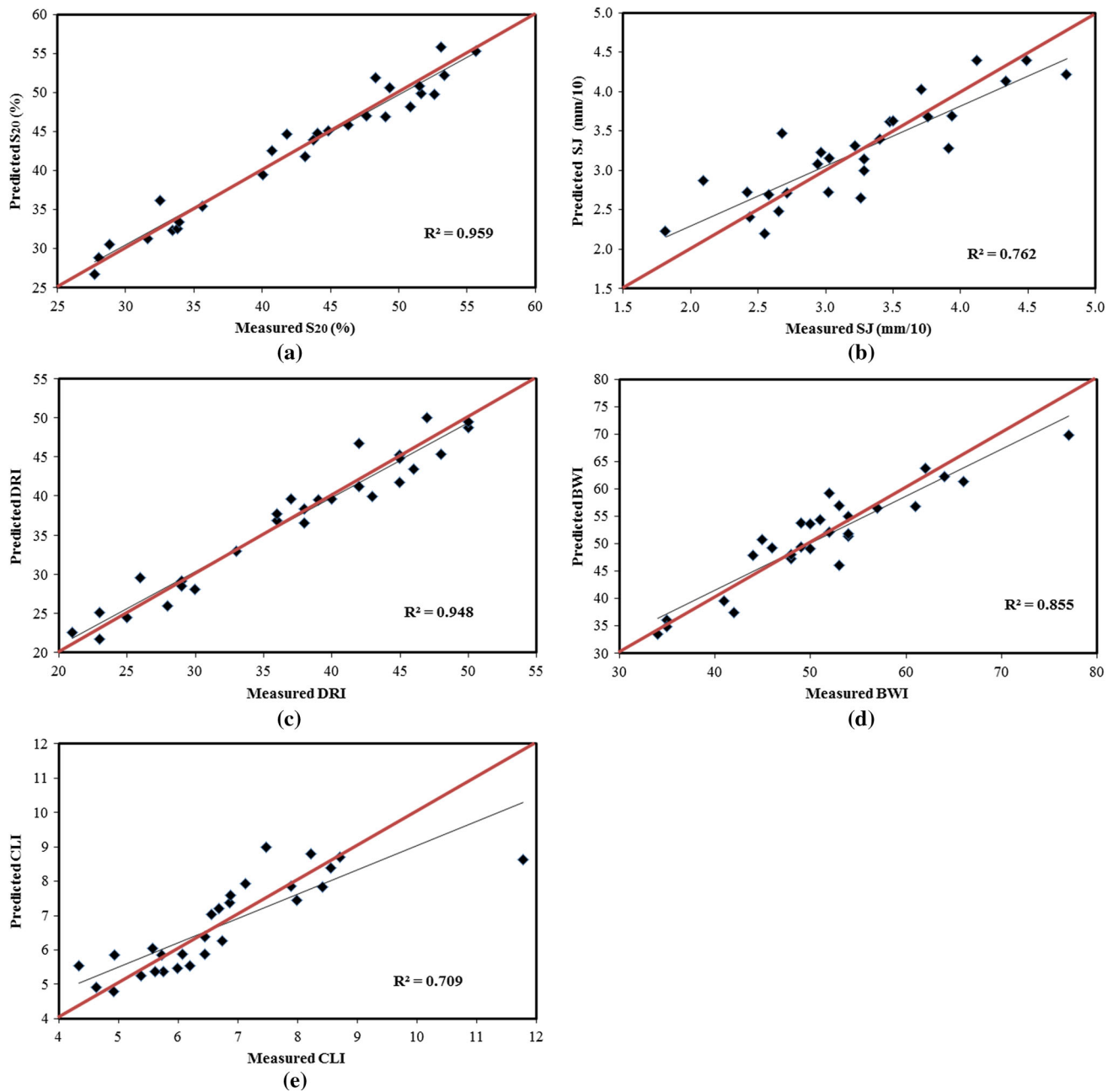


Fig. 16 Graphs of the predicted drillability parameters from petrographic features versus the measured drillability parameters: S_{20} (a), SJ (b), DRI (c), BWI (d), and CLI (e)

etration of drilling bits and cutting tools in rocks. Eventually, it is suggested conducting the petrographical method proposed in this work, by a slight modification in mineralogical indices, also on predicting the drillability properties of other rock types.

Acknowledgements The authors gratefully acknowledge Mr. Filip Dahl (SINTEF, Norway) for his useful documents and guidance upon the NTNU/SINTEF rock drillability test procedures and apparatus.

References

- Aligholi S, Khajavi R, Razmara M (2015) Automated mineral identification algorithm using optical properties of crystals. *Comput Geosci* 85:175–183
- Aligholi S, Lashkaripour GR, Khajavi R, Razmara M (2017a) Automatic mineral identification using color tracking. *Pattern Recognit* 65:164–174
- Aligholi S, Lashkaripour GR, Ghafoori M (2017b) Strength/Brittleness classification of igneous intact rocks based on basic physical and dynamic properties. *Rock Mech Rock Eng* 50(1):45–65

- Altindag R (2010) Assessment of some brittleness indexes in rock drilling efficiency. *Rock Mech Rock Eng* 43:361–370
- Anon (1995) The description and classification of weathered rocks for engineering purposes. Geological Society Engineering Group Working Party Report. *Q J Eng Geol* 28:207–242
- Asmussen P, Conrad O, Günther A, Kirsch M, Riller U (2015) Semi-automatic segmentation of petrographic thin section images using a “seeded-region growing algorithm” with an application to characterize weathered subarkose sandstone. *Comput Geosci* 83:89–99
- Aydin A (2009) ISRM Suggested method for determination of the Schmidt hammer rebound hardness: revised version. *Int J Rock Mech Min Sci* 46:627–634
- Azimian A, Ajalloeian R, Fatehi L (2014) An empirical correlation of uniaxial compressive strength with P-wave velocity and point load strength index on marly rocks using statistical method. *Geotech Geol Eng* 32(1):205–214
- Barla G, Pelizza S (2000) TBM tunneling in difficult ground conditions, Proceedings of GeoEng 2000. Proceedings of the International Conference on Geotechnical & Geological Engineering. Technomic Publishing Company, Lancaster, Melbourne, pp 329–354
- Barton N (2000) TBM tunnelling in jointed and faulted rock. A.A. Balkema, Rotterdam. ISBN 9058093417
- Blindheim OT, Grov E, Nilsen B (2002) The effect of mixed face conditions (MFC) on hard rock TBM performance. In: AITES-ITA word tunnel congress, Sydney, pp 24–32
- Bruland A (1998a) Hard rock tunnel boring. PhD thesis, Department of Civil and Transport Engineering, NTNU, Trondheim, Norway
- Bruland A (1998b) Prediction model for performance and costs, in Norwegian TBM Tunnelling, Publication No. 11, Norwegian Tunnelling Society
- Bruland A (1998c) Hard rock tunnel boring—Vol. 1—Background and discussion. NTNU Trondheim, p 49
- Bruland A (1998d) Hard rock tunnel boring: drillability—test methods. Project report 13A-98, NTNU Trondheim
- Bruland A (1998e) Hard rock tunnel boring: drillability—statistics of drillability test results. Project report 13C-98, NTNU Trondheim
- Dahl F (2003) DRI, BWI, CLI Standards. NTNU, Angleggsdrift, Trondheim, Norway, p 20
- Dahl F, Grov E, Breivik T (2007) Development of a new direct test method for estimating cutter life, based on the Sievers’ J miniature drill test. *Tunn Undergr Space Technol* 22:106–116
- Dahl F, Bruland A, Grov E, Nilsen B (2010) Trademarking the NTNU/SINTEF drillability test indices. *Tunn Tunn Int* (June), 44–46
- Dahl F, Bruland A, Jakobsen PD, Nilsen B, Grov E (2012) Classifications of properties influencing the drillability of rocks, based on the NTNU/SINTEF test method. *Tunn Undergr Space Technol* 28:150–158
- Davis JC (1973) Statistics and data analysis in geology. Wiley, New York, p 550
- Deere DU, Miller RP (1966) Engineering classification and index properties for intact rocks. Tech Rep no. AFNL-TR-65-116, Air Force Weapons Laboratory, New Mexico, p 300
- Dursun AE, Gokay MK (2016) Cuttability assessment of selected rocks through different brittleness values. *Rock Mech Rock Eng* 49(4):1173–1190
- Ellecosta P, Schneider S, Kasling H, Thuro K (2015) Hardness—a new method for characterising the interaction of TBM disc cutters and rocks?. In: Proceedings of the 13th congress on rock mechanics, ISRM Congress 2015. In-novation in applied and theoretical rock mechanics, Palais des Congres der Montre al, Canada, Paper 688, p 10. (ISBN: 978-1926872-25-4)
- Ersoy A, Waller MD (1995) Textural characterisation of rocks. *Eng Geol* 39:123–136
- Espallargas N, Jakobsen PD, Langmaack L, Macias FJ (2015) Influence of corrosion on the abrasion of cutter steels used in TBM tunnelling. *Rock Mech Rock Eng* 48(1):261–275
- Farrokh E, Rostami J, Laughton C (2011) Analysis of unit supporting time and support installation time for Open TBMs. *Rock Mech Rock Eng* 44(4):431–445
- Fueten F, Mason J (2007) An artificial neural net assisted approach to editing edges in petrographic images collected with the rotation polarizer stage. *Comput Geosci* 33:1176–1188
- Gong QM, Zhao J (2009) Development of a rock mass characteristics model for TBM penetration rate prediction. *Int J Rock Mech Min Sci* 46(1):8–18
- Hashemnejad A, Ghafoori M, Tarigh Azali S (2016) Utilizing water, mineralogy and sedimentary properties to predict LCPC abrasivity coefficient. *Bull Eng Geol Environ* 75(2):841–851
- Hassanpour J (2009) Investigation of the effect of engineering geological parameters on TBM performance and Modifications to existing prediction models. Ph.D. Thesis, Tarbiat Modares University, Tehran, Iran
- Hassanpour J, Rostami J, Tarigh Azali S, Zhao J (2014) Introduction of an empirical TBM cutter wear prediction model for pyroclastic and mafic igneous rock; a case history of Karaj water conveyance tunnel, Iran. *Tunn Undergr Space Technol* 43(2014):222–231
- Howarth DF, Rowlands JC (1987) Quantitative assessment of rock texture and correlation with drillability and strength properties. *Rock Mech Rock Eng* 20:57–85
- Hugman RH, Friedman M (1979) Effects of texture and composition on mechanical behavior of experimentally deformed carbonate rocks. *Am Assoc Pet Geol Bull* 63(9):1478–1489
- ISRM (1981) Rock characterization, testing and monitoring. Pergamon, Oxford, ISRM suggested methods, p 211
- ISRM (1985) Suggested methods for determining point load strength. *Int J Rock Mech Min Sci Geomech Abstr* 22(2):51–60
- ISRM (2007) The complete ISRM suggested methods for rock characterization, testing and monitoring: 1974–2006. In: Ulusay R, Hudson JA (eds) Suggested methods prepared by the commission on testing methods. International Society for Rock Mechanics. Compilation Arranged by the ISRM Turkish National Group, Ankara, p 293
- Izadi H, Sadri J, Mehran NA (2015) A new intelligent method for minerals segmentation in thin sections based on a novel incremental color clustering. *Comput Geosci* 81:38–52
- Jakobsen PD, Bruland A, Dahl F (2013) Review and assessment of the NTNU/SINTEF Soil Abrasion Test (SATTM) for determination of abrasiveness of soil and soft ground. *Tunn Undergr Space Technol* 37:107–114
- Jin X (2012) Filed Nov. 14, 2007, and issued Sept. 4 (2012) Segmentation-based image processing system. U.S. Patent 8,260,048
- Jung J, Brousse R (1959) Classification modale des roches éruptive.s: roches éruptive.s utilisant les données fournies par le compteur de points. Paris: Masson & Cie
- Kahraman S, Fener M, Kasling H, Thuro K (2016) The influences of textural parameters of grains on the LCPC abrasivity of coarse-grained igneous rocks. *Tunn Undergr Space Technol* 58:216–223
- Karakus M, Kumral M, Kilic O (2005) Predicting elastic properties of intact rocks from index tests using multiple regression modeling. *Int J Rock Mech Min Sci* 42:323–330
- Katz O, Reches Z, Roegiers JC (2000) Evaluation of mechanical rock properties using a Schmidt hammer. *Int J Rock Mech Min Sci* 37:723–728
- Larsen ES, Miller FS (1935) The Rosiwal method and the modal determination of rocks. *Am Mineral* 20:260–273
- Lashkaripour GR (2002) Predicting mechanical properties of mudrock from index parameters. *Bull Eng Geol Environ* 61(1):73–77

- Liu Z, Shao J, Xu W, Wu Q (2015) Indirect estimation of unconfined compressive strength of carbonate rocks using extreme learning machine. *Acta Geotech* 10(5):651–663
- Macias FJ, Jakobsen PD, Bruland A (2014a) Rock mass variability and TBM prediction. ISRM Regional Symposium - EUROCK 2014, 27–29 May, Vigo, Spain
- Macias FJ, Jakobsen PD, Seo Y, Bruland A (2014b) Influence of rock mass fracturing on the net penetration rates of hard rock TBMs. *Tunn Undergr Space Technol* 44:108–120
- Macias FJ, Dahl F, Bruland A (2016) New rock abrasivity test method for tool life assessments on hard rock tunnel boring: the rolling indentation abrasion test (RIAT). *Rock Mech Rock Eng* 49(5):1679–1693
- Middleton A, Freestone IC, Leese MN (1985) Textural analysis of ceramic thin sections: evaluation of grain sampling procedures. *Archaeometry* 27(1):64–74
- Johannessen O, Jacobsen K, Ronn PE, Moe, HL (1995) Project Report 2C-95 tunnelling costs for drill and blast. NTNU Trondheim, Department of Building and Construction Engineering
- Moradzadeh M, Cheshomi A, Ghafoori M, TrighAzali S (2016) Correlation of equivalent quartz content, Slake durability index and Is50 with Cerchar abrasiveness index for different types of rock. *Int J Rock Mech Min Sci* 86:42–47
- Nilsen B, Dahl F, Holzhauser J, Raleigh P (2007) The new test methodology for estimating the abrasiveness of soils for TBM tunnelling. In: Rapid excavation and tunneling conference (RETC), pp 104–116
- NTH (1983) Hard Rock Tunnel Boring, Project Report 1-83. Div. of Construction Engineering, Trondheim, Norwegian Institute of Technology, p 94
- Petruk W (1989) Short course on image analysis applied to mineral and earth sciences. Mineralogical Association of Canada, Ottawa
- Prikryl R (2006) Assessment of rock geomechanical quality by quantitative rock fabric coefficients: limitations and possible source of misinterpretations. *Eng Geol* 87:149–162
- Reedy CL (2006) Review of digital image analysis of petrographic thin sections in conservation research. *J Am Inst Conserv* 45(2):127–146
- Rostami J (1997) Development of a force estimation model for rock fragmentation with disc cutters through theoretical modeling and physical measurement of crushed zone pressure. Ph. D. Thesis, Colorado School of Mines, Golden, Colorado, USA, p. 249
- Rostami J, Ozdemir L, Bruland A, Dahl F (2005) Review of issues related to Cerchar abrasivity testing and their implications on geotechnical investigations and cutter cost estimates. In: Proceedings of the RETC, pp 738–751
- Rostami J, Ghasemi A, Gharahbagh E, Dogruoz C, Dahl F (2014) Study of dominant factors affecting Cerchar abrasivity index. *Rock Mech Rock Eng* 47(5):1905–1919
- Selmer-Olsen R, Lien R (1960) Bergartens borbartnet og sprengbarhet, *Teknisk Ukeblad*, 34, Oslo, pp 3–11
- Shalabi F, Cording EJ, Al-Hattamleh OH (2007) Estimation of rock engineering properties using hardness tests. *Eng Geol* 90:138–147
- Shorey PR, Barat D, Das MN, Mukherjee KP, Singh B (1984) Schmidt hammer rebound data for estimation of large scale in situ coal strength. *Int J Rock Mech Min Sci Geomech Abstr* 21:39–42
- Sievers H (1950) Die Bestimmung des Bohrwiderstandes von Gesteinen, *Glückauf* 86: 37/38, pp 776–784. Glückauf G.M.B.H., Essen
- Streckeisen A (1976) To each plutonic rock its proper name. *Earth Sci Rev* 12:12–33
- Tandon SR, Gupta V (2013) The control of mineral constituents and textural characteristics on the petrophysical & mechanical (PM) properties of different rocks of the Himalaya. *Eng Geol* 153:125–143
- The Science of Rock Mechanics. Part I. The Strength Properties of Rocks. In: Series on Rock and Soil Mechanics, 2nd edn, vol. 1 (1971/73), No. 2. Trans Tech Publications, Clausthal
- Thuro K (1997) Drillability Prediction: Geological Influences in Hard Rock Drill and Blast Tunneling, vol 86. Springer, Geol Rundsch, pp 426–438
- Thuro K, Plinninger RJ (2003) Hard rock tunnel boring, cutting, drilling and blasting: rock parameters for excavatability. In: Proceedings of the 10th ISRM Int. Congress on Rock Mechanics, Johannesburg, South Africa, pp 1227–1234
- Tugrul A, Zarif IH (1999) Correlation of mineralogical and textural characteristics with engineering properties of selected granitic rocks from Turkey. *Eng Geol* 51:303–317
- Ulusay R, Tureli K, Ider MH (1994) Prediction of engineering properties of a selected litharenite sandstone from its petrographic characteristics using correlation and multivariate statistical techniques. *Eng Geol* 38(1–2):135–157
- Villeneuve MC (2008) Examination of geological influence on machine excavation of highly stressed tunnels in massive hard rock. PhD thesis. Queen's University, Kingston
- Vincent L (1993) Morphological grayscale reconstruction in image analysis: applications and efficient algorithms. *IEEE Trans Image Process* 2(2):176–201
- von Matern N, Hjelmer A (1943) Forsök med pagrus (“Tests with Chippings”), *Medelände nr. 65*, Statens vaginstitut, Stockholm, pp 65. (English summary, pp 56–60)
- Yagiz S (2002) Development of rock fracture and brittleness indices to quantify the effects of rock mass features and toughness in the CSM model basic penetration for hard rock tunneling machines. Ph.D. Thesis, Department of Mining and Earth Systems Engineering, Colorado School of Mines, Golden, Colorado, USA, p 289
- Yagiz S (2008) Utilizing rock mass properties for predicting TBM performance in hard rock condition. *Tunn Undergr Space Technol* 23(3):326–339
- Yagiz S (2011) P-wave velocity test for assessment of geotechnical properties of some rock materials. *Bull Mater Sci* 34(4):947–953
- Yarali O, Kahraman S (2011) The drillability assessment of rocks using the different brittleness values. *Tunn Undergr Space Technol* 26:406–414
- Yilmaz I, Yuksek G (2009) Prediction of the strength and elasticity modulus of gypsum using multiple regression, ANN, and ANFIS models. *Int J Rock Mech Min Sci* 46(4):803–810
- Zare S (2007) Prediction model and simulation tool for time and costs of drill and blast tunnelling. PhD thesis, Department of Civil and Transport Engineering, NTNU, Trondheim, Norway
- Zare S, Bruland A (2013) Applications of NTNU/SINTEF drillability indices in hard rock tunneling. *Rock Mech Rock Eng* 46:179–187
- Zare S, Bruland A, Rostami J (2016) Evaluating D&B and TBM tunnelling using NTNU prediction models. *Tunn Undergr Space Technol* 59:55–64
- Zhao K, Janutolo M, Barla G (2012) A completely 3D model for the simulation of mechanized tunnel excavation. *Rock Mech Rock Eng* 45(4):475–497
- Zhou Y, Starkey J, Mansinha L (2004) Segmentation of petrographic images by integrating edge detection and region growing. *Comput Geosci* 30:817–831